Carbon Dioxide Capture for Storage in Deep Geologic Formations – Results from the CO_2 Capture Project

Geologic Storage of Carbon Dioxide with Monitoring and Verification

Volume 2

Elsevier Internet Homepage – http://www.elsevier.com
Consult the Elsevier homepage for full catalogue information on all books, major reference works, journals, electronic products and services.

Elsevier Titles of Related Interest

AN END TO GLOBAL WARMING
L.O. Williams
ISBN: 0-08-044045-2, 2002

FUNDAMENTALS AND TECHNOLOGY OF COMBUSTION
F. El-Mahallawy, S. El-Din Habik
ISBN: 0-08-044106-8, 2002

GREENHOUSE GAS CONTROL TECHNOLOGIES: 6TH INTERNATIONAL CONFERENCE
John Gale, Yoichi Kaya
ISBN: 0-08-044276-5, 2003

MITIGATING CLIMATE CHANGE: FLEXIBILITY MECHANISMS
T. Jackson
ISBN: 0-08-044092-4, 2001

Related Journals:
Elsevier publishes a wide-ranging portfolio of high quality research journals, encompassing the energy policy, environmental, and renewable energy fields. A sample journal issue is available online by visiting the Elsevier web site (details at the top of this page). Leading titles include:

Energy Policy
Renewable Energy
Energy Conversion and Management
Biomass & Bioenergy
Environmental Science & Policy
Global and Planetary Change
Atmospheric Environment
Chemosphere – Global Change Science
Fuel, Combustion & Flame
Fuel Processing Technology

All journals are available online via ScienceDirect: www.sciencedirect.com

To Contact the Publisher
Elsevier welcomes enquiries concerning publishing proposals: books, journal special issues, conference proceedings, etc. All formats and media can be considered. Should you have a publishing proposal you wish to discuss, please contact, without obligation, the publisher responsible for Elsevier's Energy program:

Henri van Dorssen
Publisher
Elsevier Ltd
The Boulevard, Langford Lane
Kidlington, Oxford
OX5 1GB, UK

Phone: +44 1865 84 3682
Fax: +44 1865 84 3931
E.mail: h.dorssen@elsevier.com

General enquiries, including placing orders, should be directed to Elsevier's Regional Sales Offices – please access the Elsevier homepage for full contact details (homepage details at the top of this page).

Carbon Dioxide Capture for Storage in Deep Geologic Formations – Results from the CO_2 Capture Project

Geologic Storage of Carbon Dioxide with Monitoring and Verification

Edited by

Sally M. Benson
Lawrence Berkeley Laboratory
Berkeley, CA,USA

and Associate Editors

Curt Oldenburg[1], Mike Hoversten[1] and Scott Imbus[2]
[1]Lawrence Berkeley National Laboratory
Berkeley, CA, USA
[2]Chevron Texaco Energy Technology Company
Bellaive, TX, USA

Volume 2

ELSEVIER
2005

Amsterdam – Boston – Heidelberg – London – New York – Oxford
Paris – San Diego – San Francisco – Singapore – Sydney – Tokyo

ELSEVIER B.V.
Radarweg 29
P.O. Box 211, 1000 AE Amsterdam
The Netherlands

ELSEVIER Inc.
525 B Street, Suite 1900
San Diego, CA 92101-4495
USA

ELSEVIER Ltd
The Boulevard, Langford Lane
Kidlington, Oxford OX5 1GB
UK

ELSEVIER Ltd
84 Theobalds Road
London WC1X 8RR
UK

First edition 2005

Library of Congress Cataloging in Publication Data
A catalog record is available from the Library of Congress.

British Library Cataloguing in Publication Data
A catalogue record is available from the British Library.

ISBN: 0-08-044570-5 (2 volume set)

Volume 1: Chapters 8, 9, 13, 14, 16, 17, 18, 24 and 32 were written with support of the U.S. Department of Energy under Contract No. DE-FC26-01NT41145. The Government reserves for itself and others acting on its behalf a royalty-free, non-exclusive, irrevocable, worldwide license for Governmental purposes to publish, distribute, translate, duplicate, exhibit and perform these copyrighted papers. EU co-funded work appears in chapters 19, 20, 21, 22, 23, 33, 34, 35, 36 and 37. Norwegian Research Council (Klimatek) co-funded work appears in chapters 1, 5, 7, 10, 12, 15 and 32.

Volume 2: The Storage Preface, Storage Integrity Preface, Monitoring and Verification Preface, Risk Assessment Preface and Chapters 1, 4, 6, 8, 13, 17, 18, 19, 20, 21, 22, 23, 24, 25, 26, 27, 28, 29, 30, 31, 32, 33 were written with support of the U.S. Department of Energy under Contract No. DE-FC26-01NT41145. The Government reserves for itself and others acting on its behalf a royalty-free, non-exclusive, irrevocable, worldwide license for Governmental purposes to publish, distribute, translate, duplicate, exhibit and perform these copyrighted papers. Norwegian Research Council (Klimatek) co-funded work appears in chapters 9, 15 and 16.

♾ The paper used in this publication meets the requirements of ANSI/NISO Z39.48-1992 (Permanence of Paper).
Printed in The Netherlands.

Carbon Dioxide Capture for Storage in Deep Geologic Formations, Volume 2
D.C. Thomas and S.M. Benson (Eds.)

Chapter 30

IMPACT OF CO_2 INJECTIONS ON DEEP SUBSURFACE MICROBIAL ECOSYSTEMS AND POTENTIAL RAMIFICATIONS FOR THE SURFACE BIOSPHERE

T.C. Onstott

Department of Geosciences, Princeton University, Princeton, NJ, USA

ABSTRACT

Based upon the calculated potential microbial power for microbial redox reactions, the most readily identified impact of CO_2 injections on the subsurface microbial communities was the reduction of one pH unit for the ground water hosted in the siliclastic reservoir. The slightly lower pH is based upon the assumption, yet to be verified, that alteration of detrital feldspars to clay in equilibrium with calcite occurs on the time scale of the injection. The power levels for many of the microbial redox reactions were generally larger than in the original ground water systems but because of this reduction of one pH unit in the ground water, microbial Fe(III) reduction reactions were significantly enhanced over the expected ambient conditions. If sufficient electron donors are available for both biotic and abiotic Fe(III) reducing reactions and sufficient Fe(III) bearing oxides are present in the aquifer (as is usually the case) then these reactions will restore the aquifer's pH to its initial, pre-injection value. CO_2 injection should cause a short-term stimulation of Fe(III) reducing communities. For long-term storage of CO_2 in siliclastic reservoirs the short-term enhancement of Fe(III) reducing microorganisms will increase the pH and most likely lead to the precipitation of various carbonates. As readily available Fe(III) is depleted it can be introduced. If this is not feasible and sulfate is not a major constituent in the ground water, then methanogenic activity will begin to dominate and the proportion of CO_2 converted to CH_4 will depend upon the H_2 and acetate fluxes.

A dolomitic or carbonate aquifer may be more severely impacted by the simulated CO_2 injection because the dissolution of the carbonate failed to restore the pH to a range that is more commensurate with the pH ranges of some of the microorganisms. If mafic igneous rocks host the groundwater and contain Fe bearing clinopyroxene, then the lower pH will automatically stimulate the release of H_2 by the oxidation of this ferrous iron to $Fe(OH)_3$. This, in turn, would lead to stimulation of methanogenic and acetogenic communities and a reduction of the injected CO_2. Fe(III) reducing microbial reactions may also be stimulated by the appearance of $Fe(OH)_3$ leading to Fe(III) reduction and an eventual increase in pH.

For rhizosphere and surface biosphere the most obvious impact would be due to a potential increase in crustal CH_4 flux for carbonate and mafic rock hosted aquifers and a decrease in H_2 flux in all cases. Since the fluxes of both gaseous species from fermentative communities in shallower, organic-rich aquitards are 10–100 times greater than the deep subsurface flux, this probably is not a showstopper.

INTRODUCTION

Liquid CO_2 injection into hydraulically tight, deep permeable formations has been proposed as a means of carbon mitigation and is used to develop oil reservoirs. The extent to which subsurface microbial communities will play a role in the long-term fate of CO_2 is not known and it may depend upon numerous factors including the abundance, diversity and relative proportions of autotrophic to heterotrophic organisms in the community, the abundance of potential electron donors (e.g. H_2, acetate and fermenters), the formation of a separate gas phase in the aquifer, the ambient temperature and pressure.

Deep subsurface microbial communities are dominated by four anaerobic, physiological types, methanogens, sulfate or sulfur reducing bacteria, fermentative anaerobes and Fe(III) reducing bacteria. These encompass the majority of subsurface species encountered to date. Their presence or absence in the 16S rDNA clone libraries can be roughly correlated with the free energy of the redox reactions they utilize for energy maintenance and the availability of the reactants in these redox reactions. The combination of energy and availability, referred to in this report as the potential microbial power, is an important parameter for gauging microbial activity. To ascertain the probable impacts of CO_2 injection upon deep subsurface microbial communities we calculated the potential microbial power for a range of ground water chemistries and temperatures, in a carbonate and siliclastic aquifer subjected to high partial pressures of CO_2.

BACKGROUND

Over the past 15 years scientists have discovered the existence of microbial communities surviving at depths to at least 3.2 km below the terrestrial land surface (kmbls.) [1]. The sessile or rock bound population density declines with depth from $\sim 10^8$ cell g^{-1} at just below the soil zone to 10^2–10^5 cell g^{-1} in solid rock at ~ 3 kmbls., whereas the planktonic cell density ranges between 10^2 and 10^6 cell ml^{-1} and exhibits a slight decline with depth (Figure 1). A majority of these microorganisms represent new species, new genera and perhaps in some cases new phyla on the microbial tree of life. Most of these deep-seated environments include autotrophic methanogens, acetogens and sulfate reducers that utilize CO_2 but struggle in an aqueous environment that is HCO_3^--poor, perhaps even limiting, Ca-rich, alkaline and usually electron-acceptor limited. Ground water dating indicates that these communities can survive for tens to hundreds of millions of years and indirect evidence suggests that they are self-sufficient in terms of nutrient and energy resources [2]. In other words, they do not necessarily rely upon downward transport of growth substrates from the surface photosphere, but are biologically and chemically isolated.

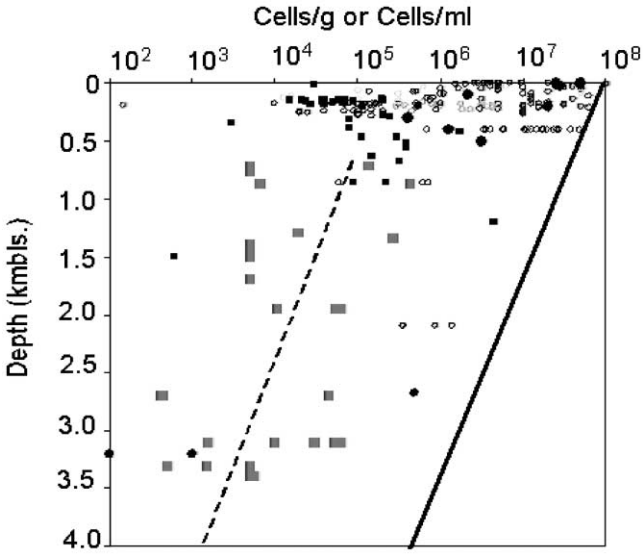

Figure 1: Cellular density as a function of depth for sediments (filled and solid circles) and ground water samples (filled and open squares) from subsurface microbial studies cited in Ref. [4]. Large open squares represent results from the fracture water in the Witwatersrand basin, South Africa (unpublished data) based upon flow cytometry analyses and large filled circles represent results from rock strata in the Witwatersrand Basin, South Africa [5]. The solid line is the least squares best fit from Parkes et al. [6] based upon marine sediment data collected up to a depth of 800 m and the dashed line is an extrapolation of that best fit to greater depths.

The biomass concentration and level of activity are controlled by temperature, water activity, porosity, permeability, substrate and trace metal concentrations, substrate availability and the free energy of the redox reactions utilized for metabolisms. Of the large number of redox reactions that are relevant to H, C, N, O, S and P cycling by microorganisms living at temperatures less than 120 °C [3], we have focused on 47 redox reactions, 42 of which are known to be associated with specific genera and five of which are abiotic (Table 1).

The microbial diversity in deep subsurface environments has begun to be well established with application of 16S rDNA analyses. This data tells us that most of the 47 redox reactions are being utilized by some member of the subsurface microbial community. Biodiversity appears to diminish dramatically with depth with some fractures in the Witwatersrand Basin possessing only one strain of microorganism. Some of the patterns that have emerged include the following:

1. For many aquifers where ambient temperatures are < 40 °C and the depths are < 500 m, members of the Proteobacteria division are common [7,8]. These include aerobic heterotrophs, methanotrophs, facultative anaerobes bacteria and chemolithotrophs. Members of the Crenarchaeota and Euryarchaeota division of the Archaea are also common in this aquifer. The Proteobacteria also appear in drilling water and mine water and therefore appear to be the dominant type of microbial contaminants.
2. The sulfate and S reducing bacteria of the δ Proteobacteria division, the Firmicutes and occasionally Archaea are common constituents of deep subsurface aquifers, [9] particularly oil reservoirs where sulfate concentrations are > 100 μM. The anaerobic hydrocarbon oxidizing sulfate reducing bacteria appear to be confined to the δ Proteobacteria division [10]. Sulfate reducing bacteria that utilize aromatic hydrocarbons, such as benzoate, do occur in injection fluids in North Sea oil fields, but because we have no information regarding the concentration of aromatic hydrocarbons from formation fluids [11] and because these particular organisms have not been found to be indigenous to the subsurface (yet) we have not included this in our modeling.
3. Thiosulfate reducing bacteria that belong to the low G + C Firmicutes group, *Fusibacter paucivorans*, are also found in oil field brines [12]. Other phylogenetically related members of the *Clostridiales* that are fermentative bacteria appear to be subterranean inhabitants capable of not just fermenting organic acids and producing H_2 but of using other electron acceptors, such as thiosulfate, in the process [13]. This would appear to be essential given that the high concentrations of H_2 typically present in the subsurface preclude derivation of ATP from straight fermentation.
4. Thermophilic, Fe(III) reducing members of Firmicutes are found in deep subsurface formations where sulfate concentrations are < 1 mM. [14,15] Fe(III) reducing members of the δ Proteobacteria division, e.g. *Geobacter metallireducens* [16] and the γ Proteobacteria domain, e.g. *Shewanella putrefaciens* [17] are found in shallow aquifers and in developed oil reservoirs [18] at mesophilic temperatures.
5. Thermophilic and hyperthermophilic members of Thermus [14] and Archaea [1] are found in deep subsurface aquifers, though rarely, and phylogenetically are closely related to hyperthermophiles and thermophiles found in surface hot springs.
6. In the case of the Witwatersrand Basin, South Africa, approximately one third of the 16S rDNA clone sequences are not closely related to sequences in the ribosomal data base and may represent new species of unknown metabolic function.

These trends have also been seen in the 16S rDNA data of petroleum reservoirs (Hinton, personal communication, 2003).

STUDY METHODOLOGY

The modeling involved the following four steps:

1. *Aquifer prior to CO_2 injection*. Geochemist workbench version 4 (Rockware Inc.) was utilized to calculate the free energy of the 47 reactions in Table 1 for three reservoir temperatures, 20, 45 and 80 °C, and for four ground water compositions (Table 2). We have restricted the maximum temperature to the upper limit for thermophiles, because we have very little evidence to date for the existence of hyperthermophilicity in the deep subsurface with the exception of Stetter et al.'s [19] discovery of hyperthermophilic Archaea associated with oil reservoirs. The four ground water types represent

TABLE 1
MICROBIALLY FACILITATED AND ABIOGENIC NON-PHOTOSYNTHETIC REDOX REACTIONS

Reaction no.	Microbial redox reaction	Classification		Example Phylla
15	$CH_4 + 2O_2 \rightarrow HCO_3^- + H^+ + H_2O$	Aerobic	Methanotrophs	β Proterobacteria: *Methylmonas*
11	Acetate $+ 2O_2 \rightarrow 2HCO_3^- + H^+$			γ Proterobacteria: *Aeromonas hydrophilia*
23	$2H_2 + O_2 \rightarrow 2H_2O$	Chemolithotrophs	Knall Gas Bacteria	β Proterobacteria: *Hydrogenophaga*
19	$2CO + O_2 + 2H_2O \rightarrow 2HCO_3^- + 2H^+$		Carboxydobacteria	α Proterobacteria: *Psuedomonas*
44	$NH_3 + 1.5O_2 \rightarrow NO_2^- + H^+ + H_2O$		Nitrifiers	β Proterobacteria: *Nitrosomonas*
46	$2NO_2^- + O_2 \rightarrow 2NO_3^-$			α Proterobacteria: *Nitrobacter*
17	$HS^- + 2O_2 \rightarrow SO_4^{2-} + H^+$		S-oxidizers	γ Proteobacteria: *Thiothrix*
16	$S_2O_3^{2-} + 2O_2 + H_2O \rightarrow 2SO_4^{2-} + 2H^+$			β Proterobacteria: *T. thioparus*
21	$S + 1.5O_2 + H_2O \rightarrow SO_4^{2-} + 2H^+$			β Proterobacteria: *T. thiooxidans*
18	$2HS^- + 2O_2 \rightarrow S_2O_3^{2-} + H_2O$			β Proterobacteria: *T. thioparus*
25	$2HS^- + O_2 + 2H^+ \rightarrow 2S + 2H_2O$			β Proterobacteria: *T. thioparus*
40	$4Fe^{2+} + O_2 + 10H_2O \rightarrow 4Fe(OH)_3 + 8H^+$		Fe-oxidizers	β Proterobacteria: *T. ferrooxidans*
47	$2Mn^{2+} + O_2 + 2H_2O \rightarrow 2MnO_2 + 4H^+$		Mn-oxidizers	β Proterobacteria: *Leptothrix*
7	$4H_2 + NO_3^- + H+ \rightarrow NH_3 + 3H_2O$	Nitrate Reducing		
1	$5H_2 + 2NO_3^- + 2H+ \rightarrow N_2 + 6H_2O$			
8	Acetate $+ NO_3^- + H_2O \rightarrow 2HCO_3^- + NH_3$			γ Proterobacteria: *Psuedomonas stutzeri*
2	Acetate $+ 1.6NO_3^- + 0.6H^+ \rightarrow 2HCO_3^- + 0.8H_2O + 0.8N_2$			Firmicutes: *Geobacillus*
4	$4CO + NO_3^- + 5H_2O \rightarrow 4HCO_3^- + NH_3 + 3H^+$			none
6	$2.5CO + NO_3^- + 2H_2O \rightarrow 2.5HCO_3^- + 1.5H^+ + 0.5N_2$			none
9	$S_2O_3^{2-} + NO_3^- + 2H_2O \rightarrow 2SO_4^{2-} + H^+ + NH_3$			β Proterobacteria: *T. denitrificans*
10	$HS^- + NO_3^- + H_2O \rightarrow SO_4^{2-} + NH_3$			β Proterobacteria: *T. denitrificans*
3	$2S + 1.5NO_3^- + 3.5H_2O \rightarrow 2SO_4^{2-} + 2.5H^+ + 1.5NH_3$			β Proterobacteria: *T. denitrificans*
45	$4Mn^{2+} + NO_3^- + 5H_2O \rightarrow 4MnO_2 + 7H^+ + NH_3$			
13	$5Fe^{2+} + NO_3^- + 12H_2O \rightarrow 5Fe(OH)3 + 9H^+ + 0.5N_2$			
14	$NO_2^- + H^+ + NH_3 \rightarrow 2H_2O + N_2$		Anaamox	Planctomycetales
39	Acetate + 4Hematite $+ 15H^+ \rightarrow 8Fe^{2+} + 8H_2O + 2HCO_3^-$	Fe(III) Reducing		Firmicutes
33	CO + Hematite $+ 3H^+ \rightarrow 2Fe^{2+} + H_2O + HCO_3^-$			none
41	H_2 + Hematite $+ 4H^+ \rightarrow 2Fe^{2+} + 3H_2O$			γ Proteobacteria: *S. putrefacians* and Crenarchaeota: *Pyrodictum islandicum*

5	$Acetate + 4MnO_2 + 7H^+ \rightarrow 4Mn^{2+} + 4H_2O + 2HCO_3^-$	Mn(IV) Reducing		Firmicutes: *B. Infernus*
28	$4H_2 + H^+ + SO_4^{2-} \rightarrow HS^- + 4H_2O$	Sulfate Reducing		Firmicutes: *Desulfotomaculum*, Euryarchaeota: *Archaeoglobus*
31	$Acetate + SO_4^{2-} \rightarrow 2HCO_3^- + HS^-$			Firmicutes: *Desulfotomaculum*, Euryarchaeota: *Archaeoglobus*
20	$4CO + SO_4^{2-} + 4H_2O \rightarrow 4HCO_3^- + HS^- + 3H^+$			δ Proteobacteria: *Desulfococcus*, Firmicutes: *Desulfotomaculum*
35	$CH_4 + SO_4^{2-} \rightarrow H_2O + HCO_3^- + HS^-$		Anaerobic Methane Oxidation	δ Proteobacteria: *Desulfosarcina* + Euryarcheota: ANME: 1&2
37	$4H_2 + H^+ + 2HCO_3^- \rightarrow Acetate + 4H_2O$	CO_2 Reducing	Acetogen	Firmicutes: *Morella thermoacetica*
32	$4H_2 + H^+ + HCO_3^- \rightarrow CH_4 + 3H_2O$		Autotrophic Methanogen	Euryarchaeota: *Methanococcus*
30	$4Formate + H^+ + H_2O \rightarrow CH_4 + 3HCO_3^-$	Fermentation	Methanogen	Euryarchaeota
36	$Acetate + H_2O \rightarrow CH_4 + HCO_3^-$		Aceticlastic Methanogen	Euryarchaeota
38	$S_2O_3^{2-} + H_2O \rightarrow SO_4^{2-} + H^+ + HS^-$		S disproportionation	
24	$S_2O_3^{2-} + 4H_2 \rightarrow 3H_2O + 2HS^-$			δ Proteobacteria: *Desulfocapsa* and Firmicutes: *Desulfotomaculum*
42	$Propanoate + 3H_2O \rightarrow Acetate + HCO_3^- + H^+ + 3H_2$		Fermenters	
26	$H_2 + S \rightarrow HS^- + H^+$	S Reducer		Eubacteria: *Thermotogales*: Thermosipho Euryarchaeota: *Thermococcus*
12	$Acetate + 4S + 4H_2O \rightarrow 5H^+ + 2HCO_3^- + 4HS^-$			Euryarchaeota: *Thermococcus*
Abiogenic Reactions				
43	$HS^- + 4Hematite + 15H^+ \rightarrow SO_4^{2-} + 8Fe^{2+} + 8H_2O$			
22	$4CO + 5H_2O \rightarrow CH_4 + 3HCO_3^- + 3H^+$		Fischer-Tropsch	
27	$3H_2 + CO \rightarrow CH_4 + H_2O$		Fischer-Tropsch	
34	$CO + 2H_2O \rightarrow HCO_3^- + H^+ + H_2$		Gas Shift Reaction	Euryarchaeota: *M. thermoautotrophicum* (reverse reaction)
29	$3H_2 + N_2 \rightarrow 2NH_3$		N_2 fixation	

Other Fe(III) bearing mineral phases modeled included $Fe(OH)_3$, Goethite and Magnetite.

the average of 200 analyses of ground water collected at depths ranging up to 3.2 kmbls. in South Africa and is the only data set with sufficient detailed analyses to permit calculation of the free energy of the reactions in Table 1. The coupling of geochemical analyses of ground water with partial equilibrium calculation of the free energy of redox reactions to determine the principal terminal electron acceptor process has been successfully applied to shallow contaminated aquifers [20]. The four ground water types include dolomitic water, low salinity meteoric water, moderate salinity water and highly saline water. The dolomitic water is typical of carbonate dominated water and in terms of major cation and anion composition is comparable to that reported for the Madison limestone and Floridian aquifers [21,22].

2. *Aquifer during CO_2 injection*. The PCO_2 was set at 200 bars, equivalent to the hydrostatic pressure at 2 kmbls. and the four ground water types were equilibrated with this high PCO_2. We assumed that CO_2 injection occurs as a separate phase. The change in PCO_2, pH and pe will impact the free energy for most of the 47 redox reactions in Table 1. The formation of a separate phase in a H_2O saturated aquifer will result in a reduction of the dissolved gas concentrations and the amount of reduction will depend upon the volume ratio of gas to fluid. We did not attempt to model this effect, because the gas concentrations in Table 1 probably reflect the formation of a separate CH_4 gas phase during depressurization. We also treated the CO_2 injection as a pulse injection so we could examine the processes that could mitigate the reduction in CO_2.
3. *Aquifer following CO_2 injection*. The final parameter variation involved dissolution of aquifer minerals by carbonic acid. For the dolomitic water dolomite and calcite was dissolved until both minerals obtained saturation and the pH and pe stabilized [22]. In the case of low salinity, moderate salinity and high salinity ground water, albite and calcite were chosen as the aquifer minerals. These two mineral phases not only appear to control major cation composition of the ground water types in South Africa but also that of saline water associated with petroleum reservoirs in the Gulf Coast [23]. The dissolution of these two minerals phases proceeded until they both attained saturation at which point pH and pe stabilized. Other minerals were allowed to precipitate during the dissolution reaction. These minerals included sulfide minerals that control trace metal concentrations, clay minerals that mitigate pH and Al concentrations, Chalcedony which controls Si concentrations, and Nahcolite that like Calcite is influenced by the PCO_2. Fe hydroxide surface protonation reactions were not utilized in the simulations at 20 °C, but their effect probably would have been to moderate the acid production of the high PCO_2.
4. To relate the free energy of the microbial redox reactions in Table 1 calculated in the first three steps to microbial activity or ATP production we made three assumptions. The first is that conservation of energy does occur during electron transport processes as first proposed by Thauer et al. [24] for anaerobic reactions occurs for all of the metabolic pathways involved in the 42 microbial redox reactions listed in Table 1. Secondly, we assumed that conversion of this chemical energy to ATP takes place with a maximum efficiency, which is equivalent to saying that a minimum chemical free energy, ΔG, is required for ATP synthesis to occur. For normal bacteria, this minimum energy is 70 kJ mol^{-1} of reactant, but under certain conditions, ATP synthesis has been observed to proceed at 20 J mol^{-1} of reactant [25] and microbial activity has been recorded to occur in the lab at $\sim$12–15 J mol^{-1} of organic reactant with syntrophic microbial consortia [26]. For the purpose of our calculations we have used a value of 20 kJ mol^{-1} as the minimum free energy required for ATP synthesis. Finally, we assumed that the maximum rate at which this energy could be accrued was given by the maximum rate of diffusion of the rate limiting reactant to the microorganism. This rate (mol cell^{-1} s^{-1}) is approximately by $4\pi DrC$, where C is the concentration of the rate limiting reactant (mol kg^{-1}), D the diffusivity of the reactant (cm^2 s^{-1}) and r the radius of the microorganism. We assumed r was 0.5 μm for all simulations. The reactant diffusivity increases with temperature according to the Stokes–Einstein relationship and the values used were from Cussler [27]. This assumption presumes that deep subsurface microorganisms are nonmotile, which is a safe assumption given their extraordinarily slow rates of growth [28,29]. The potential microbial power (J cell^{-1} s^{-1}) for a specific microbial redox reaction is equal to $4\pi DrC\Delta G$. The rate needs to be at least equivalent to the demand by the microorganism as required for its maintenance energy demand in order for the pathway to be viable. In the case of a mesophilic nitrifying bacterium, this maintenance demand is on the order of 1.7×10^{-19} kJ cell^{-1} s^{-1}. In the case of a mesophilic methanogen the maintenance demand is on the order of 1.4×10^{-19} kJ cell^{-1} s^{-1} (Colwell, personal communication, 2004).

TABLE 2
GEOCHEMICAL COMPOSITION OF FOUR DEEP GROUND WATER TYPES USED IN SIMULATIONS

Ground water type	**pH**	**pe**	***T*** **(°C)**	**TOC (gfw = 12)**	**DOC (gfw = 12)**	**DIC (gfw = 44)**	**Acetate**	**Formate**	**Propionate**	**F**	**Cl**
Anions (ppm)											
Dol	7.62	0.55	26	17.50	5.00	153.33	0.45	1.80	0.01	2.30	26
LowS	8.86	−3.03	41	1.00	1.50	29.99	0.65	0.09	0.05	3.63	102
ModS	8.78	−3.90	43	8.35	5.14	25.05	1.41	0.20	0.12	2.20	1,274
Brine	8.05	−3.89	44	8.83	13.95	8.52	2.98	1.11	0.67	0.93	13,680
	NO_2^-	SO_4^{2-}	HS^-	$S_2O_3^{2-}$	Br	NO_3^-	PO_4^{2-}	Total P as PO_4^{2-}	I		
Dol	0.005	79.08	20.39	0.01	0.59	0.54	0.010	1.07	0.48		
LowS	0.004	14.97	26.17	0.43	1.12	0.04	0.018	0.03			
ModS	0.060	34.42	15.53	0.87	6.50	0.16	0.011	2.08	0.87		
Brine	0.069	120.93	20.72	0.68	76.02	0.14	0.024	6.16	3.22		
Cations and trace metals (ppm)											
	NH_3 (gfw = 14)	Li	Na	Mg	K	Rb	Ca	Sr	Ba	Al	Si
Dol	0.02	0.01	16	29.62	1.41	0.003	57	0.169	0.131	0.468	7.38
LowS	0.18	0.07	78	0.07	2.11	0.181	11	0.156	0.017	0.061	15.45
ModS	0.42	0.49	555	2.93	6.67	0.071	197	4.202	0.649	0.267	9.28
Brine	0.45	2.85	3,876	134.41	46.99	0.826	3,619	96.828	15.172	0.261	8.12
	Mn	Fe	Mo	Cr	Co	Ni	Cu	Zn	As	W	U
Dol	0.042	0.309	0.020	0.037	0.007	0.020	0.008	0.030	0.0250	0.0296	0.0220
LowS	0.004	0.201	0.182	0.004	0.002	0.015	0.038	0.008	0.0115	0.0779	0.0239
ModS	0.746	0.328	0.050	0.019	0.002	0.011	0.007	0.068	0.0293	0.0726	0.0349
Brine	2.527	8.063		0.020	0.004	0.052	0.024	0.037	0.0574	0.0868	0.1027
Dissolved gases (μM)											
	H_2	He	Ar	N_2	CH_4	C_2H_6	C_3H_8	iso-C_4	*n*-C_4	CO	
Dol	0.97	1.30	7.00	350.00	104.91	0.00	0.00	0.00	0.00	0.37	
LowS	0.13	162.49	9.64	1907.54	1150.95	62.84	12.98	0.25	0.88	0.34	
ModS	181.47	441.44	62.63	4019.32	6223.95	109.68	13.14	0.29	1.74	11.44	
Brine	515.20	1082.57	148.86	3625.57	10,740.75	603.77	55.36	0.46	5.25	69.94	

For example, 200 mmol of ATP are required to produce 1 g of anaerobic bacteria (wet weight) if acetate or CO_2 is the carbon substrate. For a cell mass of 10^{-12} g dry weight, this means that 2×10^{-13} mol of ATP or 1.4×10^{-11} kJ are required to produce one cell. If the potential microbial power for aceticlastic, sulfate reduction was $\sim 10^{-11}$ J s^{-1} $cell^{-1}$, then sufficient energy would be accrued after $\sim 2 \times 10^3$ s for a single cell. If the biomass concentration of the ground water and aquifer was 4×10^9 cells kg^{-1} like that reported for the Middendorf Aquifer by Phelps et al. [28] and all the cells in the ground water were utilizing this one reaction (reaction (31) in Table 1) at a rate of 10^{-16} mol $s^{-1}cell^{-1}$, then the steady state rate of HCO_3^- production in the aquifer would be 4×10^{-7} mol kg^{-1} s^{-1} or 35 mmol kg^{-1} day^{-1}. This estimated rate is far greater than the ~ 10 and 0.001 μmol kg^{-1} day^{-1} sulfate reduction rates determined by Phelps et al. [28] which were based upon $^{35}SO_4$ measurements for the former and geochemical reaction rates for the Middendorf aquifer calibrated by ^{14}C ages for the latter.

Part of the discrepancy may be explained if just a small portion of the biomass is active, sulfate reducing bacteria. Regardless, the expression, $4\pi DrC\Delta G$, is considered a maximum potential for microbial power, as it ignores enzyme inhibition by competitive species or reactions and the transport rate across the cellular membrane. In the case of solid reactants, such as S and Fe(III) and Mn(IV) bearing oxides, we have assumed that the limiting reactant is the aqueous phase, not the solid phase, which clearly cannot be true all the time. We have also not corrected for the minimum concentration required for an enzyme to function or to be expressed. Nevertheless, we feel that the potential microbial power values for the different redox reactions can be used to assess the relative importance of one type of metabolism versus another.

RESULTS AND DISCUSSION

Initial Conditions

The four ground water types exhibit the following trends with increasing salinity and temperature (deeper ground water tends to be hotter and more saline):

1. The pe becomes more negative. As reliable dissolved O_2 measurements are difficult to make when concentrations are close to the detection limit of 0.03 mM, we have utilized the fO_2 predicted by the pe as our estimate of the dissolved O_2 for the model simulations.
2. With the exception of the dolomite water the pH decreases.
3. Sulfate concentrations increase whereas sulfide concentrations are relatively uniform with the possible exception of the dolomite water.
4. The Fe and Mn concentrations increase.
5. Dissolved reduced gases and hydrocarbons increase.
6. Trace levels of nitrate and nitrite are present throughout with the highest nitrate concentration associated with the dolomite water.
7. The ammonia concentration increases.
8. The concentration of organic acids increases, whereas the concentration of inorganic carbon decreases.

These trends, particularly the increasing dissolved organic acids and reducing potential with depth or temperature is consistent with observations of pore water and ground water from basins where organic matter is far more abundant than our South African aquifers. With the dolomite, moderate salinity and highly saline ground water, calcite is saturated and the concentration of the decreasing DIC is a direct reflection of the increasing Ca concentrations and elevated pH. If the pH were to remain constant during CO_2 injection, the Ca concentrations would remove a large fraction of the CO_2 and precipitate it as calcite. The degree to which the microorganisms would facilitate such a process is a subject for the next stage of investigation (see Recommendations). The first and most important question to be answered by the modeling is as follows. Do any of the microbial redox reactions that yield negative free energies for our subsurface ground water types become positive under the conditions anticipated to occur with CO_2 injection? This would be considered a detrimental impact on those subsurface microorganisms relying upon those specific redox reactions.

The free energy and potential microbial power calculations for the four types of ground water (Tables 3 and 4) provide a baseline against which to compare the community structure inferred from the 16S rDNA results and the simulated geochemical changes associated with CO_2 injection. The free energy calculations revealed the following:

1. The two microbial redox reactions that are the most obviously relevant to CO_2 injection are the CO_2 reducing methanogenesis and acetogenesis reactions (reactions (32) and (37) in Table 3 and Figure 2). The free energy for both the reactions decrease with increasing temperature and are marginally exothermic in the dolomitic and low salinity ground water type where dissolved H_2 concentrations are <1 μM (Table 2), but are exothermic in the moderate and high salinity water where H_2 concentrations are >100 μM.
2. For all four ground water types the ammonia oxidizing and the Mn oxidizing reactions were all positive regardless of temperature (reactions (44)–(47) in Table 3 and Figure 2). The implication is that in order for these reactions to proceed the O_2 concentrations must be much higher than is typical even for microaerophilic ground water. This is also consistent with the absence of nitrifying and Mn oxidizing organisms from the 16S rDNA results for aquifers. Nitrifying bacteria have been found associated with the more oxygenated drilling water. Anaerobic ammonia oxidation by reduction of nitrite, the anammox reaction (reaction (14) in Table 3 and Figure 2) is energetically favorable in all four ground water types, but the microorganisms associated with this reaction belong to the order of the *Planctomycetales* [30] and the 16S rDNA signatures of this order have yet to be identified in the deep subsurface, although the anammox reaction has been detected in shallow marine sediments [31,32].
3. Conversely Mn reduction (reaction (5) in Table 3 and Figure 2) and nitrate reduction (reactions (1)–(4), (6)–(10) and (13)) possessed highly negative free energies. Of the nitrate reducing reactions, those yielding N_2 as the product (reactions (1), (2), (6) and (13) in Table 3 and Figure 1) were more exothermic than those yielding ammonia (reactions (3), (4) and (7)–(10) in Table 3 and Figure 2).
4. Despite the extremely low concentrations of dissolved O_2 predicted by measured pe for the four ground water types, aerobic reactions (reactions (11), (15)–(19), (21), (23) and (25) in Table 3 and Figure 2) still retained highly negative free energies. These free energies increase with temperature as fO_2 increases. The most energetic reaction is acetate oxidation (reaction (11) in Table 3 and Figure 2) followed by CH_4, thiosulfate, CO, HS^-, S, H_2 and the least exothermic aerobic reaction is oxidation of HS^- to S (reaction (25) in Table 3 and Figure 2).
5. Reduction of S compounds to HS^- (reactions (12), (24), (26), (28), (31) and (35) in Table 3 and Figure 2) was energetically favorable. The most exothermic reaction was the reduction of S to HS^- by acetate (reaction (12) in Table 3 and Figure 2). The free energies of S reduction reactions with acetate increased with increasing temperature, whereas those with H_2 decreased with increasing temperature.
6. The anaerobic oxidation of CH_4 coupled to the reduction of SO_4^{2-} to HS^- (reaction (35) in Table 3 and Figure 2) is the least exothermic S reducing reaction. This reaction has been detected in shallow, marine sediments and methane clathrates where it appears to require the syntrophic activity of two microorganisms, one of which is a H_2 utilizing sulfate reducing bacteria and one of which is a CO_2 reducing methanogen. The methanogen is believed to be reversibly oxidizing CH_4 by reaction (32) in Tables 1 and 3. This can only occur if the H_2 concentration is low enough for the free energy of reaction (32) to exceed $+20$ kJ mol^{-1} [33]. The free energy yields for reaction (35), therefore, are not germane even though they would appear to be favorable. Accordingly, Table 3 indicates that only the low salinity ground water at high temperature would be energetically favorable for anaerobic CH_4 oxidation.
7. Although anaerobic oxidation of hydrocarbon by sulfate reduction was not specifically modeled, the free energy for these reactions is slightly greater than that of the anaerobic CH_4 oxidation.
8. The free energy for reduction of hematite to Fe^{2+} is pH and temperature dependent with the reaction favored for low pH and low temperature (reactions (39) and (41) in Table 3 and Figure 2). This holds true for the other Fe(III) oxides as well. In this report, we have restricted the analysis to hematite under the presumption that amorphous $Fe(OH)_3$ and goethite would be the first phases to be reduced leaving hematite as the sole, remaining, Fe(III) oxide for deep, anaerobic environments. Microbial reduction of magnetite would require even lower pH values than is typical of these environments. In the absence of a reaction that would regenerate $Fe(OH)_3$ our model would suggest that microbial Fe(III) reduction would be restricted to mesophilic environments for ground water with pH $\sim$ 7.5. Because microbial Fe(III) reduction by either acetate or H_2 raises the pH of the environment this represents a severe

TABLE 3
FREE ENERGY (KJ MOL^{-1}) FOR REDOX/MICROBIAL REACTIONS IN DOLOMITIC, LOW SALINITY, MODERATE SALINITY AND HIGHLY SALINE GROUND WATER AT 20, 45 AND 80 °C

Microbial redox reactions	1. Do 20	2. Do 45	3. Do 80	4. LS 20	5. LS 45	6. LS 80	7. MS 20	8. MS 45	9. MS 80	10. Br 20	11. Br 45	12. Br 80
(1) $5H_2 + 2NO_3^- + 2H^+ \rightarrow N_2 + 6H_2O$	−983	−957	−920	−923	−892	−848	−1225	−993	−961	−1249	−1015	−984
(2) Acetate + $1.6NO_3^- + 0.6H^+ \rightarrow 2HCO_3^- + 0.8H_2O + 0.8N_2$	−749	−744	−739	−736	−731	−725	−896	−740	−735	−907	−750	−747
(3) $2S + 1.5NO_3^- + 3.5H_2O \rightarrow 2SO_4^{2-} + 2.5H^+ + 1.5NH_3$	−700	−700	−699	−697	−699	−702	−840	−698	−702	−833	−691	−690
(4) $4CO + NO_3^- + 5H_2O \rightarrow 4HCO_3^- + NH_3 + 3H^+$	−655	−645	−627	−673	−665	−654	−855	−707	−703	−884	−732	−728
(5) Acetate + $4MnO_2 + 7H^+ \rightarrow 4Mn^{2+} + 4H_2O + 2HCO_3^-$	−648	−631	−609	−627	−609	−584	−708	−567	−540	−790	−642	−626
(6) $2.5CO + NO_3^- + 2H_2O \rightarrow 2.5HCO_3^- + 1.5H^+ + 0.5N_2$	−567	−559	−547	−576	−569	−559	−724	−597	−591	−740	−612	−608
(7) $4H_2 + NO_3^- + H^+ \rightarrow NH_3 + 3H_2O$	−535	−516	−488	−490	−468	−439	−678	−547	−526	−700	−565	−543
(8) Acetate + $NO_3^- + H_2O \rightarrow 2HCO_3^- + NH_3$	−497	−494	−490	−487	−485	−484	−594	−491	−492	−608	−503	−502
(9) $S_2O_3^{2-} + NO_3^- + 2H_2O \rightarrow 2SO_4^{2-} + H^+ + NH_3$	−463	−458	−444	−468	−465	−462	−565	−466	−463	−560	−460	−455
(10) $HS^- + NO_3^- + H_2O \rightarrow SO_4^{2-} + NH_3$	−448	−441	−432	−437	−430	−423	−525	−429	−422	−529	−432	−422
(11) Acetate + $2O_2 \rightarrow 2HCO_3^- + H^+$	−264	−295	−336	−179	−203	−234	−166	−158	−186	−130	−126	−150
(12) Acetate + $4S + 4H_2O \rightarrow 5H^+ + 2HCO_3^- + 4HS^-$	−264	−295	−336	−179	−203	−234	−166	−158	−186	−130	−126	−150
(13) $5Fe^{2+} + NO_3^- + 12H_2O \rightarrow 5Fe(OH)_3 + 9H^+ + 0.5N_2$	−272	−294	−323	−324	−349	−385	−388	−347	−382	−372	−333	−365
(14) $NO_2^- + H^+ + NH_3 \rightarrow 2H_2O + N_2$	−297	−293	−287	−291	−285	−275	−358	−292	−284	−358	−293	−287
(15) $CH_4 + 2O_2 \rightarrow HCO_3^- + H^+ + H_2O$	−242	−271	−310	−158	−180	−209	−142	−136	−161	−102	−101	−122
(16) $S_2O_3^{2-} + 2O_2 + H_2O \rightarrow 2SO_4^{2-} + 2H^+$	−230	−259	−290	−160	−182	−212	−137	−132	−156	−82	−83	−102
(17) $HS^- + 2O_2 \rightarrow SO_4^{2-} + H^+$	−215	−242	−278	−128	−147	−172	−98	−96	−115	−52	−55	−70

(18) $2HS^- + 2O_2 \rightarrow S_2O_3^{2-} + H_2O$	−200	−225	−266	−97	−112	−132	−58	−60	−74	−21	−26	−37
(19) $2CO + O_2 + 2H_2O \rightarrow 2HCO_3^- + 2H^+$	−211	−223	−236	−182	−191	−202	−214	−187	−198	−203	−177	−188
(20) $4CO + SO_4^{2-} + 4H_2O \rightarrow 4HCO_3^- + HS^- + 3H^+$	−207	−203	−194	−236	−236	−231	−330	−278	−281	−355	−300	−306
(21) $S + 1.5O_2 + H_2O \rightarrow SO_4^{2-} + 2H^+$	−175	−200	−234	−118	−137	−163	−99	−99	−121	−58	−63	−81
(22) $4CO + 5H_2O \rightarrow CH_4 + 3HCO_3^- + 3H^+$	−180	−174	−163	−206	−203	−195	−286	−237	−235	−304	−254	−254
(23) $2H_2 + O_2 \rightarrow 2H_2O$	−151	−158	−167	−91	−93	−94	−125	−107	−110	−111	−94	−95
(24) $S_2O_3^{2-} + 4H_2 \rightarrow 3H_2O + 2HS^-$	−102	−91	−67	−85	−73	−56	−192	−154	−145	−201	−162	−154
(25) $2HS^- + O_2 + 2H^+ \rightarrow 2S + 2H_2O$	−80	−83	−89	−22	−20	*−18*	*3*	*7*	*12*	*14*	*16*	*22*
(26) $H_2 + S \rightarrow HS^- + H^+$	−76	−79	−83	−45	−46	−47	−63	−53	−55	−55	−47	−48
(27) $3H_2 + CO \rightarrow CH_4 + H_2O$	−90	−78	−58	−69	−55	−33	−153	−117	−102	−166	−129	−115
(28) $4H_2 + H^+ + SO_4^{2-} \rightarrow HS^- + 4H_2O$	−87	−74	−55	−53	−38	−16	−153	−117	−104	−170	−133	−121
(29) $3H_2 + N_2 \rightarrow 2NH_3$	−87	−74	−55	−57	−44	−29	−131	−100	−90	−150	−115	−102
(30) $4Formate + H^+ + H_2O \rightarrow CH_4 + 3HCO_3^-$	−77	−69	−60	−47	−37	−24	−63	−44	−33	−91	−69	−61
(31) $Acetate + SO_4^{2-} \rightarrow 2HCO_3^- + HS^-$	−49	−53	−58	−51	−55	−62	−68	−62	−70	−79	−71	−80
(32) $4H_2 + H^+ + HCO_3^- \rightarrow CH_4 + 3H_2O$	−61	−45	−24	−24	*−5*	*21*	−108	−77	−58	−120	−87	−69
(33) $CO + Hematite + 3H^+ \rightarrow 2Fe^{2+} + H_2O + HCO_3^-$	−54	−41	−20	−37	−23	*−1*	−58	−34	−15	−70	−46	−28
(34) $CO + 2H_2O \rightarrow HCO_3^- + H^+ + H_2$	−30	−32	−35	−46	−49	−54	−44	−40	−44	−46	−42	−46
(35) $CH_4 + SO_4^{2-} \rightarrow H_2O + HCO_3^- + HS^-$	−27	−29	−32	−30	−33	−37	−44	−41	−46	−51	−46	−52
(36) $Acetate + H_2O \rightarrow CH_4 + HCO_3^-$	−22	−24	−26	−21	−23	−25	−24	−21	−24	−28	−25	−28
(37) $4H_2 + H^+ + 2HCO_3^- \rightarrow Acetate + 4H_2O$	−38	−22	*2*	*−3*	*17*	*46*	−84	−55	−33	−92	−62	−41
(38) $S_2O_3^{2-} + H_2O \rightarrow SO_4^{2-} + H^+ + HS^-$	*−15*	*−17*	*−12*	−32	−35	−40	−39	−36	−41	−31	−29	−33
(39) $Acetate + 4Hematite + 15H^+ \rightarrow 8Fe^{2+} + 8H_2O + 2HCO_3^-$	−59	*−12*	*55*	*35*	*90*	*167*	*30*	*78*	*152*	*−5*	*46*	*114*
(40) $4Fe^{2+} + O_2 + 10H_2O \rightarrow 4Fe(OH)_3 + 8H^+$	*24*	*−10*	−57	*19*	*−15*	−63	*55*	*13*	−31	*91*	*46*	*6*
(41) $H_2 + Hematite + 4H^+ \rightarrow 2Fe^{2+} + 3H_2O$	−24	*−8*	*14*	*8*	*27*	*53*	*−13*	*6*	*30*	−24	*−4*	*18*
(42) $Propanoate + 3H_2O \rightarrow Acetate + HCO_3^- + H^+ + 3H_2$	*23*	*10*	*−9*	*−6*	−22	−44	*56*	*35*	*17*	*63*	*41*	*24*

(*continued*)

TABLE 3
CONTINUED

Microbial redox reactions	1. Do 20	2. Do 45	3. Do 80	4. LS 20	5. LS 45	6. LS 80	7. MS 20	8. MS 45	9. MS 80	10. Br 20	11. Br 45	12. Br 80
(43) $HS^- + 4Hematite + 15H^+ \rightarrow SO_4^{2-} + 8Fe^{2+} + 8H_2O$	*− 10*	*41*	*112*	*86*	*145*	*229*	*99*	*140*	*222*	*74*	*117*	*195*
(44) $NH_3 + 1.5O_2 \rightarrow NO_2^- + H^+ + H_2O$	*157*	*130*	*99*	*211*	*190*	*163*	*302*	*232*	*210*	*342*	*267*	*246*
(45) $4Mn^{2+} + NO_3^- + 5H_2O \rightarrow 4MnO_2 + 7H^+ + NH_3$	*151*	*138*	*118*	*139*	*123*	*99*	*114*	*76*	*48*	*182*	*139*	*124*
(46) $2NO_2^- + O_2 \rightarrow 2NO_3^-$	*151*	*140*	*124*	*194*	*186*	*174*	*253*	*203*	*194*	*271*	*220*	*212*
(47) $2Mn^{2+} + O_2 + 2H_2O \rightarrow 2MnO_2 + 4H^+$	*192*	*168*	*136*	*224*	*203*	*175*	*271*	*205*	*177*	*330*	*258*	*238*

The reactions are ordered from most negative to positive with respect to the free energy for the dolomite ground water at 20 °C. The microbial reaction numbers and column heading numbers refer to Figure 2. Values in italics are > -20 kJ mol^{-1} and therefore are not considered to be viable for microbial metabolism.

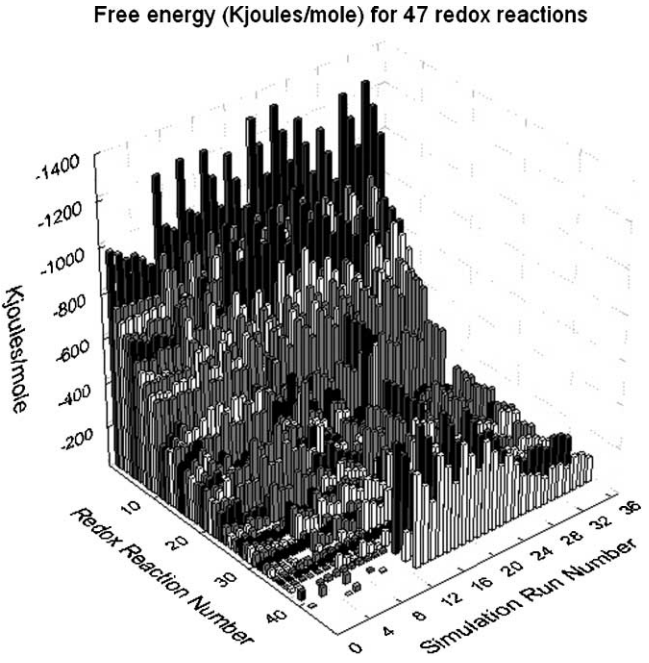

Figure 2: Free energy in kJ mol^{-1} for microbial reactions for four different types of ground water and aquifers under ambient conditions at 25, 45 and 80 °C (Simulation Run Numbers 1–12), during simulated CO_2 injection (Simulation Run Numbers 13–24), and during post-injection equilibration with aquifer minerals (Simulation Run Numbers 24–36), based upon data in Tables 3, 5 and 7.

restriction unless the aquifer is buffered to lower pH or an acid producing reaction occurs at a comparable rate.

9. The free energy for oxidation of Fe^{2+} to $Fe(OH)_3$ is also pH and temperature dependent with the reaction favored for high temperatures and high pH (reactions (13) and (40) in Table 3 and Figure 2). Fe^{2+} oxidation is weakly favored even for the minute amounts of dissolved O_2 present in our simulations. Fe^{2+} oxidation by nitrate, however, is strongly exothermic even for trace amounts of nitrate.
10. Of the organic fermentation reactions formate fermentation to CH_4 and CO_2 (reaction (30) in Table 3 and Figure 2) was the most exothermic, followed by acetate fermentation to CH_4 and CO_2 (reaction (36) in Table 3 and Figure 2) and propionate fermentation to acetate, CO_2 and H_2 (reaction (42) in Table 3 and Figure 2). The free energy for the formate reaction decreased with increasing temperature. The free energy for the acetate fermentation was remarkably constant at ~ -25 kJ mol^{-1} regardless of temperature or ground water type. The free energy for propionate fermentation increased with decreasing temperature and was only microbially favored for the high temperature, low salinity water where the dissolved H_2 concentrations were <0.1 μM. Inorganic fermentation of thiosulfate, or thiosulfate disproportionation, is marginally favorable and sensitive to the pH of the ground water with the free energy increasing as the pH increases. The free energy for formation of acetate from CO_2 and H_2 (reaction (37) in Table 3 and Figure 2) was slightly greater than that of acetate fermentation to CH_4 and CO_2 with the exception of the low salinity water with H_2 concentrations ~ 0.1 μM. This suggests that if μM concentrations of H_2 are maintained then the conversion of CO_2 to CH_4 via acetogenesis and aceticlastic methanogenesis is viable. The production of H_2 by fermentation of propionate (or for that matter benzoate or butyrate) is not energetically

favorable unless the H_2 concentrations ~ 0.1 μM. In other words, organic fermentative production of H_2 will not sustain the conversion of CO_2 to CH_4 for the conditions encountered in the deep subsurface and alternative abiotic reactions are required to do so.

11. Abiotic conversion of CO to H_2 and CO_2 or the Gas shift reaction (reaction (34) in Table 3 and Figure 2) represents a possible source of H_2, is favorable even for the highly saline water with the highest dissolved H_2 concentrations and its free energy is greater than that of acetogenesis. A competing reaction for consumption of CO, however, is the abiotic conversion of CO to CH_4 and CO_2 or the Fischer–Tropsch reaction (reaction (22) in Table 3 and Figure 2). This is energetically favorable for all ground water types and has a greater free energy than the Gas shift reaction, but its free energy decreases with increasing temperature. This reaction is most favored for the highly saline ground water probably because of the lower HCO_3^- and pH of this ground water. This suggests that if the CO_2 produced by this reaction is converted to carbonate, then the Fischer–Tropsch reaction may compete with microbial conversion of CO_2 to methane. The abiotic conversion of H_2 and N_2 to NH_3 is favorable for all four ground water types, becomes less favorable with increasing temperature consistent with observations regarding metamorphic N_2 [34], but is strongly favored for environments where H_2 concentrations are high. The rates for the Gas shift, Fischer–Tropsch and ammonia generation reactions are unknown and at the temperatures modeled in this report depend upon the catalyst available (e.g. metal oxides or sulfides).
12. The normally rapid and abiotic reduction of hematite by oxidation of HS^- to SO_4^{2-} (reaction (43) in Table 3 and Figure 2) is also not favored because of the high pH of these ground water types. The reaction becomes slightly less positive if goethite or amorphous $Fe(OH)_3$ is considered, but this reaction is extremely sensitive to the pH regardless of the choice of Fe(III) oxides and for this pH range the free energy is close to zero or positive.

The potential microbial power calculations revealed that the most exothermic reactions were not the most powerful reactions. The microbial redox reactions were ordered in Table 4 and Figure 3 to reflect their importance and this revealed the following:

1. Many of the H_2 oxidizing reactions, such as the reduction of S and SO_4^{2-} to HS^- (reactions (1) and (4) in Table 4 and Figure 3), the abiotic production of NH_3 (reaction (2) in Table 4 and Figure 3), methanogenesis and acetogenesis (reactions (7) and (12) in Table 4 and Figure 3) were the most powerful reactions despite the low free energy yields for some of these reactions. This directly corresponded to the high H_2 concentration as the power varied by four orders of magnitude from the dolomite water, 5×10^{-16} kJ cell^{-1} s^{-1}, to the highly saline water 5×10^{-12} J cell^{-1} s^{-1}, and with diffusivity as the power increases by a factor of two from 20 to 80 °C.
2. The anaerobic methane oxidation reaction (reaction (3) in Table 4 and Figure 3) is the third most powerful reaction despite its low free energy yield for highly saline water and its power increases by two orders of magnitude from the dolomite water, 5×10^{-14} kJ cell^{-1} s^{-1}, to the highly saline water, 5×10^{-12} kJ cell^{-1} s^{-1}. This is a reflection of the high concentrations and diffusivities of its reactants. As mentioned above, however, because the free energy of reaction (7) is negative, anaerobic methane oxidation via reverse methanogenesis cannot proceed.
3. Acetate oxidation coupled with the reduction of MnO_2 to Mn^{2+}, and reduction of S and SO_4^{2-} to HS^- (reactions (5), (10) and (13) in Table 4 and Figure 3) yields high potential power, 5×10^{-14} to 5×10^{-13} kJ cell^{-1} s^{-1}, because of their high free energies and the amount and diffusivity of acetate.
4. CO consuming reactions (reactions (6), (8), (9) and (11) in Table 4 and Figure 3), such as the Fischer–Tropsch reaction, are quite powerful reactions for the highly saline water. Their power values increase by three orders of magnitude from the dolomite water, 5×10^{-17} kJ cell^{-1} s^{-1}, to the highly saline water, 5×10^{-13} kJ cell^{-1} s^{-1}, and like the H_2 consuming reactions the value depends upon the CO concentration.
5. In the low salinity to highly saline ground water all of the nitrate-reducing reactions (reactions (14)–(22) and (28) in Table 4 and Figure 3) were nitrate limited and the annamox reaction nitrite limited (reaction (25) in Table 4 and Figure 3). In the dolomite water, however, the electron donor was limiting. Because these reactions yielded the greatest free energy, however, the power of nitrate reducing reactions ranged from 5×10^{-15} to 5×10^{-13} kJ cell^{-1} s^{-1}. These power values are comparable to those for the reduction of Fe(III) oxides (reactions (39) and (41) in Table 4 and Figure 3). The potential microbial power for Fe^{2+} oxidation by nitrate (reaction (28) in Table 4 and Figure 3) and reduction of hematite (reactions (30)

TABLE 4
POTENTIAL MICROBIAL POWER (5000 KJ CELL^{-1} S^{-1}) FOR FOUR TYPES OF GROUND WATER AT 20, 45 AND 80 °C

Microbial redox reactions	1. Do 20	2. Do 45	3. Do 80	4. LS 20	5. LS 45	6. LS 80	7. MS 20	8. MS 45	9. MS 80	10. Br 20	11. Br 45	12. Br 80
(1) $H_2 + S \rightarrow HS^- + H^+$	-1.8×10^{12}	-3.2×10^{12}	-5.8×10^{12}	-1.5×10^{13}	-2.5×10^{13}	-4.4×10^{13}	-2.8×10^{10}	**-4.0×10^{10}**	-6.9×10^{10}	-6.9×10^{10}	**-9.8×10^{10}**	-1.7×10^{09}
(2) $3H_2 + N_2 \rightarrow 2NH_3$	-6.8×10^{13}	-9.9×10^{13}	-1.3×10^{12}	-6.1×10^{14}	-7.9×10^{14}	-9.1×10^{14}	-1.9×10^{10}	-2.5×10^{10}	-3.8×10^{10}	-6.2×10^{10}	-8.0×10^{10}	-1.2×10^{09}
(3) $CH_4 + SO_4^{2-} \rightarrow H_2O + HCO_3^- + HS^-$	**-2.1×10^{11}**	-4.0×10^{11}	-7.3×10^{11}	-4.2×10^{11}	**-7.8×10^{11}**	-1.5×10^{10}	-1.3×10^{10}	**-1.9×10^{10}**	-3.7×10^{10}	-3.9×10^{10}	**-5.9×10^{10}**	-1.1×10^{09}
(4) $4H_2 + H^+ + SO_4^{2-} \rightarrow HS^- + 4H_2O$	-5.1×10^{13}	-7.5×10^{13}	-9.7×10^{13}	-4.3×10^{14}	-5.1×10^{14}		-1.7×10^{10}	**-2.2×10^{10}**	-3.3×10^{10}	-5.3×10^{10}	**-6.9×10^{10}**	-1.1×10^{09}
(5) Acetate $+ 4MnO_2 + 7H^+ \rightarrow 4Mn^{2+} + 4H_2O + 2HCO_3^-$	**-3.1×10^{11}**	-5.3×10^{11}	-8.7×10^{11}	-4.6×10^{11}	**-7.5×10^{11}**	-1.2×10^{10}	-9.4×10^{11}	**-1.3×10^{10}**	-2.0×10^{10}	-2.1×10^{10}	**-2.9×10^{10}**	-4.7×10^{10}
(6) $3H_2 + CO \rightarrow CH_4 + H_2O$	-7.1×10^{13}	-1.0×10^{12}	-1.4×10^{12}	-7.4×10^{14}	-9.9×10^{14}	-1.0×10^{13}	-1.7×10^{11}	-2.2×10^{11}	-3.2×10^{11}	-1.3×10^{10}	-1.7×10^{10}	-2.5×10^{10}
(7) $4H_2 + H^+ + HCO_3^- \rightarrow CH_4 + 3H_2O$	-3.6×10^{13}	-4.6×10^{13}	-4.1×10^{13}	-1.9×10^{14}			-1.2×10^{10}	**-1.4×10^{10}**	-1.8×10^{10}	-1.3×10^{10}	**-1.5×10^{10}**	-2.1×10^{10}
(8) $4CO + SO_4^{2-} + 4H_2O \rightarrow 4HCO_3^- + HS^- + 3H^+$	-2.2×10^{13}	-3.7×10^{13}	-6.1×10^{13}	-2.2×10^{13}	-3.8×10^{13}	-6.4×10^{13}	-9.2×10^{12}	-1.3×10^{11}	-2.2×10^{11}	-6.9×10^{11}	**-9.8×10^{11}**	-1.7×10^{10}
(9) $4CO + 5H_2O \rightarrow CH_4 + 3HCO_3^- + 3H^+$	-2.0×10^{13}	-3.2×10^{13}	-5.1×10^{13}	-1.9×10^{13}	-3.2×10^{13}	-5.4×10^{13}	-8.0×10^{12}	-1.1×10^{11}	-1.9×10^{11}	-5.9×10^{11}	-8.3×10^{11}	-1.4×10^{10}
(10) Acetate $+ 4S + 4H_2O \rightarrow 5H^+ + 2HCO_3^- + 4HS^-$	**-1.3×10^{11}**	-2.5×10^{11}	-4.8×10^{11}	-1.3×10^{11}	**-2.5×10^{11}**	-4.8×10^{11}	-2.2×10^{11}	**-3.5×10^{11}**	-7.0×10^{11}	-3.5×10^{11}	**-5.6×10^{11}**	-1.1×10^{10}
(11) $CO +$ Hematite $+ 3H^+ \rightarrow 2Fe^{2+} + H_2O + HCO_3^-$	-2.4×10^{13}	-3.0×10^{13}	-2.6×10^{13}	-1.4×10^{13}	-1.4×10^{13}		-6.5×10^{12}	-6.4×10^{12}		-5.5×10^{11}	**-6.0×10^{11}**	-6.1×10^{11}
(12) $4H_2 + H^+ + 2HCO_3^- \rightarrow$ Acetate $+ 4H_2O$	-2.2×10^{13}	-2.2×10^{13}					-9.4×10^{11}	**-1.0×10^{10}**	-1.1×10^{10}	-4.8×10^{11}	**-5.5×10^{11}**	-6.1×10^{11}
(13) Acetate $+ SO_4^{2-} \rightarrow 2HCO_3^- + HS^-$	-2.4×10^{12}	-4.4×10^{12}	-8.3×10^{12}	-3.7×10^{12}	**-6.8×10^{12}**	-1.3×10^{11}	-9.1×10^{12}	-1.4×10^{11}	-2.6×10^{11}	-2.1×10^{11}	**-3.2×10^{11}**	-6.0×10^{11}
(14) $4CO + NO_3^- + 5H_2O \rightarrow 4HCO_3^- + NH_3 + 3H^+$	-7.1×10^{13}	-1.2×10^{12}	-2.0×10^{12}	-6.2×10^{13}	-1.1×10^{12}	-1.8×10^{12}	-2.4×10^{11}	**-3.4×10^{11}**	-5.7×10^{11}	-2.5×10^{11}	-3.5×10^{11}	-5.9×10^{11}
(15) $2.5CO + NO_3^- + 2H_2O \rightarrow 2.5HCO_3^- + 1.5H^+ + 0.5N_2$	-9.9×10^{13}	-1.6×10^{12}	-2.8×10^{12}	-8.5×10^{13}	-1.5×10^{12}	-2.5×10^{12}	-2.1×10^{11}	**-2.9×10^{11}**	-4.8×10^{11}	-2.1×10^{11}	-2.9×10^{11}	-4.9×10^{11}

(*continued*)

TABLE 4
CONTINUED

Microbial redox reactions	1. Do 20	2. Do 45	3. Do 80	4. LS 20	5. LS 45	6. LS 80	7. MS 20	8. MS 45	9. MS 80	10. Br 20	11. Br 45	12. Br 80
(16) $S_2O_3^{2-} + NO_3^- + 2H_2O \rightarrow 2SO_4^{2-} + H^+ + NH_3$	-2.2×10^{13}	-3.7×10^{13}	-6.1×10^{13}	-5.3×10^{12}	$\mathbf{-8.9 \times 10^{12}}$	-1.5×10^{11}	-2.1×10^{11}	$\mathbf{-2.9 \times 10^{11}}$	-4.8×10^{11}	-2.1×10^{11}	-2.9×10^{11}	-4.9×10^{11}
(17) $4H_2 + NO_3^- + H^+ \rightarrow NH_3 + 3H_2O$	$\mathbf{-3.1 \times 10^{12}}$	-5.2×10^{12}	-8.5×10^{12}	-3.9×10^{13}	-6.3×10^{13}	-1.0×10^{12}	-1.9×10^{11}	-2.6×10^{11}	-4.2×10^{11}	-2.0×10^{11}	-2.7×10^{11}	-4.4×10^{11}
(18) Acetate $+ NO_3^- + H_2O \rightarrow 2HCO_3^- + NH_3$	$\mathbf{-2.4 \times 10^{11}}$	-4.1×10^{11}	-7.0×10^{11}	-4.5×10^{12}	$\mathbf{-7.7 \times 10^{12}}$	-1.3×10^{11}	-1.4×10^{11}	-2.3×10^{11}	-3.9×10^{11}	-1.7×10^{11}	-2.4×10^{11}	-4.0×10^{11}
(19) $5H_2 + 2NO_3^- + 2H^+ \rightarrow N_2 + 6H_2O$	$\mathbf{-4.6 \times 10^{12}}$	-7.7×10^{12}	-1.3×10^{11}	-4.5×10^{12}	$\mathbf{-7.5 \times 10^{12}}$	-1.2×10^{11}	-1.3×10^{11}	-2.1×10^{11}	-3.4×10^{11}	-1.7×10^{11}	-2.4×10^{11}	-3.9×10^{11}
(20) $2S + 1.5NO_3^- + 3.5H_2O \rightarrow 2SO_4^{2-} + 2.5H^+ + 1.5NH_3$	$\mathbf{-5.7 \times 10^{11}}$	-9.6×10^{11}	-1.7×10^{10}	-4.2×10^{12}	$\mathbf{-7.3 \times 10^{12}}$	-1.2×10^{11}	-1.6×10^{11}	-2.2×10^{11}	-3.8×10^{11}	-1.6×10^{11}	-2.2×10^{11}	-3.7×10^{11}
(21) Acetate $+ 1.6NO_3^- + 0.6H^+ \rightarrow 2HCO_3^- + 0.8H_2O + 0.8N_2$	$\mathbf{-3.6 \times 10^{11}}$	-6.2×10^{11}	-1.1×10^{10}	-4.3×10^{12}	$\mathbf{-7.3 \times 10^{12}}$	-1.2×10^{11}	-1.3×10^{11}	-2.2×10^{11}	-3.7×10^{11}	-1.6×10^{11}	-2.2×10^{11}	-3.7×10^{11}
(22) $HS^- + NO_3^- + H_2O \rightarrow SO_4^{2-} + NH_3$	$\mathbf{-5.5 \times 10^{11}}$	-9.1×10^{11}	-1.6×10^{10}	-4.0×10^{12}	$\mathbf{-6.7 \times 10^{12}}$	-1.1×10^{11}	-1.5×10^{11}	-2.1×10^{11}	-3.4×10^{11}	-1.5×10^{11}	-2.1×10^{11}	-3.4×10^{11}
(23) $CO + 2H_2O \rightarrow HCO_3^- + H^+ + H_2$	-3.3×10^{14}	-5.9×10^{14}	-1.1×10^{13}	-4.2×10^{14}	-7.9×10^{14}	-1.5×10^{13}	-1.2×10^{12}	-1.9×10^{12}	-3.5×10^{12}	-9.0×10^{12}	-1.4×10^{11}	-2.5×10^{11}
(24) Acetate $+ H_2O \rightarrow CH_4 + HCO_3^-$	-1.1×10^{12}	-2.0×10^{12}	-3.7×10^{12}	-1.6×10^{12}	-2.8×10^{12}	-5.2×10^{12}	-3.2×10^{12}	-4.8×10^{12}	-9.1×10^{12}	-7.4×10^{12}	-1.1×10^{11}	-2.1×10^{11}
(25) $NO_2^- + H^+ + NH_3 \rightarrow 2H_2O + N_2$	-9.1×10^{13}	-1.5×10^{12}	-2.7×10^{12}	-3.8×10^{13}	-5.2×10^{13}	-1.1×10^{12}	-5.5×10^{12}	-7.6×10^{12}	-1.2×10^{11}	-8.3×10^{12}	-1.1×10^{11}	-1.9×10^{11}
(26) $S_2O_3^{2-} + 4H_2 \rightarrow 3H_2O + 2HS^-$	-4.9×10^{14}	-7.4×10^{14}	-9.2×10^{14}	-6.8×10^{14}	-9.9×10^{14}	-1.3×10^{13}	-8.4×10^{12}	-1.1×10^{11}	-1.8×10^{11}	-6.6×10^{12}	-9.0×10^{12}	-1.4×10^{11}
(27) $4Formate + H^+ + H_2O \rightarrow CH_4 + 3HCO_3^-$	$\mathbf{-5.9 \times 10^{12}}$	-9.1×10^{12}	-1.4×10^{11}	-1.8×10^{13}	-2.5×10^{13}	-2.8×10^{13}	-5.2×10^{13}	-6.0×10^{13}	-7.8×10^{13}	-3.7×10^{12}	-4.8×10^{12}	-7.1×10^{12}
(28) $5Fe^{2+} + NO_3^- + 12H_2O \rightarrow 5Fe(OH)_3 + 9H^+ + 0.5N_2$	$\mathbf{-3.2 \times 10^{12}}$	-5.7×10^{12}	-1.1×10^{11}	-5.9×10^{13}	-1.1×10^{12}	-2.0×10^{12}	-2.2×10^{12}	-3.3×10^{12}	-6.2×10^{12}	-2.1×10^{12}	-3.2×10^{12}	-5.9×10^{12}
(29) $S_2O_3^{2-} + H_2O \rightarrow SO_4^{2-} + H^+ + HS^-$				-6.6×10^{13}	-1.2×10^{12}	-2.5×10^{12}	-1.7×10^{12}	-2.7×10^{12}	-5.1×10^{12}	-1.0×10^{12}	-1.6×10^{12}	-3.0×10^{12}
(30) Acetate $+ 4Hematite + 15H^+ \rightarrow 8Fe^{2+} + 8H_2O + 2HCO_3^-$	-2.9×10^{12}											
(31) $H_2 + Hematite + 4H^+ \rightarrow 2Fe^{2+} + 3H_2O$	-1.4×10^{12}									-6.2×10^{11}		

(32) Propionate + $3H_2O \rightarrow$ Acetate + $HCO_3^- + H^+ + 3H_2$					-1.4×10^{13}	-5.1×10^{13}						
(33) $2CO + O_2 + 2H_2O \rightarrow 2HCO_3^- + 2H^+$	-2.4×10^{61}	-4.3×10^{54}	-7.7×10^{46}	-2.1×10^{70}	-3.7×10^{64}	-6.6×10^{56}	-2.5×10^{74}	-3.6×10^{67}	-6.5×10^{59}	-2.3×10^{77}	-3.4×10^{70}	-6.1×10^{62}
(34) $2H_2 + O_2 \rightarrow 2H_2O$	-1.7×10^{61}	-3.1×10^{54}	-5.4×10^{46}	-1.0×10^{70}	-1.8×10^{64}	-3.1×10^{56}	-1.4×10^{74}	-2.1×10^{67}	-3.6×10^{59}	-1.3×10^{77}	-1.8×10^{70}	-3.1×10^{62}
(35) Acetate + $2O_2 \rightarrow 2HCO_3^- + H^+$	-1.5×10^{61}	-2.9×10^{54}	-5.5×10^{46}	-1.0×10^{70}	-2.0×10^{64}	-3.8×10^{56}	-9.6×10^{75}	-1.5×10^{67}	-3.0×10^{59}	-7.5×10^{78}	-1.2×10^{70}	-2.4×10^{62}
(36) $CH_4 + 2O_2 \rightarrow HCO_3^- + H^+ + H_2O$	-1.4×10^{61}	-2.6×10^{54}	-5.0×10^{46}	-9.1×10^{71}	-1.7×10^{64}	-3.4×10^{56}	-8.2×10^{75}	-1.3×10^{67}	-2.6×10^{59}	-5.9×10^{78}	-9.8×10^{71}	-2.0×10^{62}
(37) $S + 1.5O_2 + H_2O \rightarrow SO_4^{2-} + 2H^+$	-1.3×10^{61}	-2.6×10^{54}	-5.1×10^{46}	-9.0×10^{71}	-1.8×10^{64}	-3.5×10^{56}	-7.6×10^{75}	-1.3×10^{67}	-2.6×10^{59}	-4.5×10^{78}	-8.1×10^{71}	-1.8×10^{62}
(38) $S_2O_3^{2-} + 2O_2 + H_2O \rightarrow 2SO_4^{2-} + 2H^+$	-1.3×10^{61}	-2.5×10^{54}	-4.7×10^{46}	-9.2×10^{71}	-1.8×10^{64}	-3.5×10^{56}	-7.9×10^{75}	-1.3×10^{67}	-2.5×10^{59}	-4.7×10^{78}	-8.1×10^{71}	-1.7×10^{62}
(39) $HS^- + 2O_2 \rightarrow SO_4^{2-} + H^+$	-1.2×10^{61}	-2.3×10^{54}	-4.5×10^{46}	-7.4×10^{71}	-1.4×10^{64}	-2.8×10^{56}	-5.6×10^{75}	-9.3×10^{68}	-1.9×10^{59}	-3.0×10^{78}	-5.3×10^{71}	-1.1×10^{62}
(40) $2HS^- + 2O_2 \rightarrow S_2O_3^{2-} + H_2O$	-1.2×10^{61}	-2.2×10^{54}	-4.3×10^{46}	-5.6×10^{71}	-1.1×10^{64}	-2.2×10^{56}	-3.4×10^{75}	-5.8×10^{68}	-1.2×10^{59}	-1.2×10^{78}	-2.5×10^{71}	-6.0×10^{63}
(41) $2HS^- + O_2 + 2H^+ \rightarrow 2S + 2H_2O$	-9.2×10^{62}	-1.6×10^{54}	-2.9×10^{46}	-2.5×10^{71}	-3.8×10^{65}							
(42) HS^- + 4Hematite + $15H^+ \rightarrow SO_4^{2-} + 8Fe^{2+} + 8H_2O$												
(43) $4Fe^{2+} + O_2 + 10H_2O \rightarrow 4Fe(OH)_3 + 8H^+$			-3.7×10^{42}			-4.1×10^{52}			-2.0×10^{50}			

Microbial redox reactions have been ordered according to their power with the most powerful reactions for the 80 °C brine appearing first. The microbial reaction numbers and column heading numbers refer to Figure 3. The power is not reported for reactions for which the free energy was > -20 kJ mol^{-1}. Values in bold represent the top 10 values.

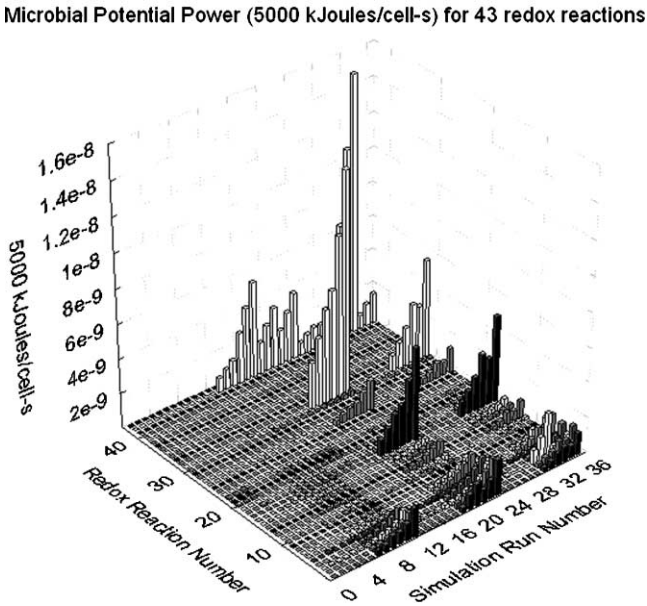

Figure 3: Free energy flux or "potential microbial power" (5000 kJ cell^{-1} s^{-1}) for four different types of ground water and aquifers under ambient conditions at 25, 45 and 80 °C (Simulation Run Numbers 1–12), during simulated CO_2 injection (Simulation Run Numbers 13–24), and during post-injection equilibration with aquifer minerals (Simulation Run Numbers 24–36), based upon values in Tables 4, 6 and 8.

and (31) in Table 4 and Figure 3) are quite similar suggesting that low levels of nitrate could contribute to sustaining microbial Fe(III) reduction at higher temperatures. It is noteworthy that two Fe(III) reducing bacteria from the deep subsurface, *Bacillus infernus* [15] and *Thermus scotoductus* [14] were both capable of nitrate reduction as well.

6. The fermentative methanogenic reactions (reactions (24) and (27) in Table 4 and Figure 3), propionate reaction (reaction (32) in Table 4 and Figure 3) and thiosulfate disproportion (reaction (26) in Table 4 and Figure 3) yielded power levels ranging from 5×10^{-16} to 5×10^{-14} kJ cell^{-1} s^{-1}.
7. All of the aerobic reactions (reactions (33)–(41) and (43) in Table 4 and Figure 3) were O_2 limited, which explains why their power levels are extremely low, $< 5 \times 10^{-43}$ kJ cell^{-1} s^{-1}, despite the high energy yield of aerobic reactions. In order for these reactions to be competitive with the above anaerobic reactions the O_2 concentrations need to be > 0.1 μM.

If we select the 10 most powerful microbial redox reactions for each ground water type we come to the following conclusions:

1. For the dolomite ground water the total potential microbial power from the top 10 reactions was 10^{-12} kJ cell^{-1} s^{-1}. The most powerful reactions are the oxidation of S and HS^- to SO_4^{2-} followed by nitrate reduction to NH_3. This appears consistent with the dominance of *Thiobacillus denitrificans* in the clone libraries from this aquifer [35]. Other potential metabolic reactions are the reduction of S to HS^-, Mn reduction and other nitrate reduction reactions. This suggests that the community would contain a diverse population of chemolithotrophs and heterotrophs and phylogenetically would probably be comprised of Proteobacteria. Because the oxidation of Fe by nitrate is among the top 10, the precipitation of $Fe(OH)_3$ is conceivable in which case microbial Fe reduction may also occur.

2. For the low salinity ground water the total potential microbial power from the top 10 reactions was 10^{-12} kJ cell^{-1} s^{-1}. The top 10 reactions were quite similar to those of the dolomite with one exception. The microbial reduction of SO_4^{2-} to HS^- was a more significant contributor to the total energy which is consistent with the appearance of SRBs in the 16S rDNA clone libraries (Kieft personal communication, 2004). It also means that the SO_4^{2-} generated by oxidation of S species to SO_4^{2-} with the reduction of nitrate could potentially fuel more sulfate reduction and form a sulfur cycle.
3. For the moderate salinity ground water the total potential microbial power from the top 10 reactions was 5×10^{-12} kJ cell^{-1} s^{-1}. The metabolic reactions are dominated by S and SO_4^{2-} reduction to HS^- and by reduction of CO_2 to methane and acetate. The change in microbial metabolic pathways is largely a reflection of the increasing H_2 concentrations. This appears consistent with the dominance of sulfate reducing members of the Firmicutes and the presence of methanogens in the clone libraries [8].
4. For the high salinity ground water the total potential microbial power from the top 10 reactions was 1.5×10^{-11} kJ cell^{-1} s^{-1}. The metabolic reactions remain dominated by S and SO_4^{2-} reduction to HS^- and by reduction of CO_2 to methane and acetate. SRBs appear to dominate the 16S rDNA clone libraries of the highly saline fracture water [36], but methanogens appear to be absent. One difference between the high salinity and moderate salinity ground water is that abiotic reactions appear competitive based upon their potential power. This appears to be consistent with isotopic data on hydrocarbons reported from these ground water types [37]. Another difference is that CO oxidation by SO_4^{2-} reduction to HS^- and by reduction of hematite appears to be competitive, but microorganisms capable of coupling these electron donors and acceptors have not been isolated to our knowledge. Finally, the highly saline water was CO_2 limited for CO_2 reducing reactions, an observation that bears some significance in terms of the injection of CO_2.
5. The microbial power for the more saline ground water types is greater than that of the dolomite and low salinity water and that power is concentrated into fewer reactions. The microbial power for the dolomite and low salinity water is more equally divided among the microbial redox reactions. This suggests that deeper, more saline ground water microbial communities are less diverse than the shallower, less saline ground water microbial communities, a trend which is borne out in the 16S rDNA clone libraries.

Injection of CO_2

The equilibration of the four ground water types with 200 bars of CO_2 decreased the pH to 2.7–3.3, and consequently increased the pe to 1–7, and dramatically increased dissolved CO_2 and HCO_3^- concentrations to 2.5–8 and 0.002–0.004 mol kg^{-1}, respectively. Solubilization of trace mineral phases affected the concentrations of trace metals and phosphate which obviously have potential impact upon microbial processes. For the purposes of this study we have focused on the first three effects, which had the following significant impact upon the acid and CO_2 producing microbial redox reactions:

1. The fermentation reactions of acetate to CH_4 and CO_2 (reaction (36) in Table 5) and propionate fermentation to acetate, CO_2 and H_2 (reaction (42) in Table 5) were no longer favorable for any of the ground water compositions. This would be a serious impediment to strictly aceticlastic methanogens, whereas the propionate reaction would be more dependent upon the $P\,H_2$.
2. The oxidation of reduced S compounds by O_2 (reactions (16)–(18), (21) and (25) in Table 5), which were marginally favorable in the highly saline ground water became endothermic with injection of the CO_2. Given that aerobic S oxidizers are not found in this ground water environment, this does not appear to be a significant perturbation.
3. Of the microbial reactions that were originally unfavorable prior to injection, the reduction of hematite to Fe^{2+} by oxidation of acetate (reaction (39) in Table 5) and H_2 (reaction (41) in Table 5) were far more exothermic due to the reduction in pH. The abiotic reduction of hematite by oxidation of HS^- (reaction (43) in Table 5) is also energetically favorable now.
4. The high CO_2 and HCO_3^- concentrations increased the free energy yield for CO_2 reducing methanogenic and acetogenic reaction (reactions (32) and (37) in Table 5). An increase in acetogenic activity may rescue the aceticlastic methanogens.
5. The aerobic oxidation of acetate (reaction (11) in Table 5) was less favorable because it is a proton and HCO_3^- producing reaction. Other acetate oxidation reactions, however, such as MnO_2 or nitrate reduction were more favorable.

TABLE 5
FREE ENERGY (KJOULE MOLE^{-1}) OF I REDOX REACTIONS FOR GROUND WATER EQUILIBRATED WITH 200 BARS OF CO_2.

Microbial redox reactions	13. Do 20	14. Do 45	15. Do 80	16. LS 20	17. LS 45	18. LS 80	19. MS 20	20. MS 45	21. MS 80	22. Br 20	23. Br 45	24. Br 80
(1) $5H_2 + 2NO_3^- + 2H^+ \rightarrow N_2 + 6H_2O$	−1246	−1122	−976	−1193	−1069	−924	−1305	−1182	−1036	−1321	−1197	−1053
(2) Acetate + $1.6NO_3^- + 0.6H^+ \rightarrow$ $2HCO_3^- + 0.8H_2O + 0.8N_2$	−907	−832	−745	−890	−815	−728	−897	−822	−735	−899	−824	−738
(3) $2S + 1.5NO_3^- + 3.5H_2O \rightarrow$ $2SO_4^{2-} + 2.5H^+ + 1.5NH_3$	−813	−747	−673	−799	−733	−655	−797	−733	−655	−797	−731	−653
(4) $4CO + NO_3^- + 5H_2O \rightarrow$ $4HCO_3^- + NH_3 + 3H^+$	−724	−653	−569	−710	−640	−553	−754	−683	−597	−777	−706	−621
(5) Acetate + $4MnO_2 + 7H^+ \rightarrow$ $4Mn^{2+} + 4H_2O + 2HCO_3^-$	−981	−895	−793	−1017	−932	−829	−966	−883	−781	−1012	−930	−837
(6) $2.5CO + NO_3^- + 2H_2O \rightarrow$ $2.5HCO_3^- + 1.5H^+ + 0.5N_2$	−634	−574	−503	−622	−562	−491	−650	−591	−519	−664	−604	−534
(7) $4H_2 + NO_3^- + H^+ \rightarrow NH_3 + 3H_2O$	−706	−631	−544	−670	−596	−507	−758	−683	−595	−772	−697	−610
(8) Acetate + $NO_3^- + H_2O \rightarrow$ $2HCO_3^- + NH_3$	−616	−566	−508	−606	−555	−496	−610	−560	−501	−614	−564	−506
(9) $S_2O_3^{2-} + NO_3^- + 2H_2O \rightarrow$ $2SO_4^{2-} + H^+ + NH_3$	−551	−501	−375	−564	−514	−456	−564	−515	−457	−560	−511	−453
(10) $HS^- + NO_3^- + H_2O \rightarrow SO_4^{2-} + NH_3$	−544	−496	−441	−538	−490	−432	−537	−489	−432	−537	−489	−432
(11) Acetate + $2O_2 \rightarrow 2HCO_3^- + H^+$	−344	−322	−438	−302	−282	−261	−101	−278	−261	−73	−71	−130
(12) Acetate + $4S + 4H_2O \rightarrow$ $5H^+ + 2HCO_3^- + 4HS^-$	−344	−322	−438	−302	−282	−261	−73	−278	−261	−73	−71	−130
(13) $5Fe^{2+} + NO_3^- + 12H_2O \rightarrow$ $5Fe(OH)_3 + 9H^+ + 0.5N_2$		−61	−73		−31	−44		−31	−42		−52	−58
(14) $NO_2^- + H^+ + NH_3 \rightarrow 2H_2O + N_2$	−355	−324	−286	−348	−317	−282	−356	−324	−289	−355	−324	−288
(15) $CH_4 + 2O_2 \rightarrow HCO_3^- + H^+ + H_2O$	−329	−306	−422	−293	−272	−250	−95	−271	−253	−66	−64	−121
(16) $S_2O_3^{2-} + 2O_2 + H_2O \rightarrow 2SO_4^{2-} + 2H^+$	−278	−257	−305	−260	−241	−221	−55	−233	−217	*−19*	*−18*	−77
(17) $HS^- + 2O_2 \rightarrow SO_4^{2-} + H^+$	−272	−252	−371	−234	−216	−197	−28	−207	−192	*4*	*4*	−56
(18) $2HS^- + 2O_2 \rightarrow S_2O_3^{2-} + H_2O$	−266	−247	−437	−209	−191	−173	−1	−180	−166	*27*	*26*	−35
(19) $2CO + O_2 + 2H_2O \rightarrow 2HCO_3^- + 2H^+$	−226	−204	−249	−203	−183	−159	−122	−200	−178	−118	−107	−123
(20) $4CO + SO_4^{2-} + 4H_2O \rightarrow 4HCO_3^-$ $+ HS^- + 3H^+$	−180	−157	−128	−172	−150	−121	−216	−194	−165	−240	−217	−189
(21) $S + 1.5O_2 + H_2O \rightarrow SO_4^{2-} + 2H^+$	−202	−191	−284	−172	−161	−151	*7*	−155	−148	*7*	*4*	−45
(22) $4CO + 5H_2O \rightarrow CH_4 + 3HCO_3^- + 3H^+$	−123	−103	−77	−114	−94	−68	−150	−130	−104	−170	−150	−124

(23) $2H_2 + O_2 \rightarrow 2H_2O$	−217	−193	−237	−183	−161	−136	−124	−201	−177	−115	−102	−117
(24) $S_2O_3^{2-} + 4H_2 \rightarrow 3H_2O + 2HS^-$	−167	−140	−37	−158	−131	−99	−247	−221	−189	−257	−230	−199
(25) $2HS^- + O_2 + 2H^+ \rightarrow 2S + 2H_2O$	−140	−123	−175	−125	−109	−92	−21	−104	−88	*−7*	*0*	−23
(26) $H_2 + S \rightarrow HS^- + H^+$	−108	−97	−119	−92	−81	−68	−58	−100	−89	−58	−51	−58
(27) $3H_2 + CO \rightarrow CH_4 + H_2O$	−109	−86	−58	−84	−61	−33	−153	−130	−102	−166	−143	−115
(28) $4H_2 + H^+ + SO_4^{2-} \rightarrow HS^- + 4H_2O$	−161	−135	−103	−132	−106	−75	−220	−194	−163	−234	−208	−178
(29) $3H_2 + N_2 \rightarrow 2NH_3$	−166	−141	−113	−148	−122	−90	−210	−185	−153	−222	−197	−167
(30) $4Formate + H^+ + H_2O \rightarrow CH_4 + 3HCO_3^-$	−102	−88	−72	−60	−47	−31	−65	−51	−36	−81	−68	−53
(31) $Acetate + SO_4^{2-} \rightarrow 2HCO_3^- + HS^-$	−72	−70	−67	−68	−66	−64	−73	−71	−69	−77	−75	−74
(32) $4H_2 + H^+ + HCO_3^- \rightarrow CH_4 + 3H_2O$	−104	−81	−52	−74	−50	−22	−154	−130	−102	−164	−141	−112
(33) $CO + Hematite + 3H^+ \rightarrow 2Fe^{2+} + H_2O + HCO_3^-$	−156	−133	−103	−162	−139	−110	−173	−151	−122	−170	−148	−121
(34) $CO + 2H_2O \rightarrow HCO_3^- + H^+ + H_2$	*−5*	*−6*	*−6*	*−10*	*−11*	*−12*	*1*	*0*	*−1*	*−1*	*−2*	*−3*
(35) $CH_4 + SO_4^{2-} \rightarrow H_2O + HCO_3^- + HS^-$	−57	−54	−51	−59	−56	−53	−67	−64	−61	−70	−68	−65
(36) $Acetate + H_2O \rightarrow CH_4 + HCO_3^-$	*−15*	*−15*	*−16*	*−9*	*−9*	*−10*	*−6*	*−7*	*−8*	*−7*	*−7*	*−8*
(37) $4H_2 + H^+ + 2HCO_3^- \rightarrow Acetate + 4H_2O$	−89	−65	−36	−65	−40	−11	−147	−123	−94	−157	−133	−104
(38) $S_2O_3^{2-} + H_2O \rightarrow SO_4^{2-} + H^+ + HS^-$	*−6*	*−5*	*66*	−26	−25	−24	−27	−26	−26	−23	−22	−21
(39) $Acetate + 4Hematite + 15H^+ \rightarrow 8Fe^{2+} + 8H_2O + 2HCO_3^-$	−515	−443	−352	−543	−473	−381	−549	−480	−392	−516	−449	−369
(40) $4Fe^{2+} + O_2 + 10H_2O \rightarrow 4Fe(OH)_3 + 8H^+$		*206*	*95*		*241*	*198*		*247*	*204*		*335*	*258*
(41) $H_2 + Hematite + 4H^+ \rightarrow 2Fe^{2+} + 3H_2O$	−151	−127	−97	−152	−128	−98	−174	−151	−121	−168	−146	−118
(42) $Propionate + 3H_2O \rightarrow Acetate + HCO_3^- + H^+ + 3H_2$	*60*	*42*	*20*	*39*	*21*	*−1*	*102*	*84*	*62*	*109*	*91*	*68*
(43) $HS^- + 4Hematite + 15H^+ \rightarrow SO_4^{2-} + 8Fe^{2+} + 8H_2O$	−443	−373	−285	−475	−407	−317	−476	−409	−323	−439	−374	−296
(44) $NH_3 + 1.5{*}O_2 \rightarrow NO_2^- + H^+ + H_2O$	*196*	*174*	*43*	*221*	*198*	*168*	*379*	*209*	*176*	*404*	*368*	*279*
(45) $4Mn^{2+} + NO_3^- + 5H_2O \rightarrow 4MnO_2 + 7H^+ + NH_3$	*364*	*330*	*284*	*411*	*377*	*333*	*398*	*322*	*280*	*398*	*367*	*331*
(46) $2NO_2^- + O_2 - > 2NO_3^-$	*153*	*140*	*54*	*166*	*152*	*134*	*260*	*147*	*128*	*274*	*250*	*193*
(47) $2Mn^{2+} + O_2 + 2H_2O \rightarrow 2MnO_2 + 4H^+$	*318*	*287*	*177*	*358*	*325*	*284*	*470*	*302*	*260*	*470*	*430*	*353*

The reactions are ordered from most negative to positive with respect to the free energy for the dolomite ground water at 20 °C. The microbial reaction numbers and column heading numbers refer to Figure 10. Values in italics are > -20 kJ mol^{-1} and therefore are not considered to be viable for microbial metabolism.

TABLE 6

POTENTIAL MICROBIAL POWER (5000 KJ CELL^{-1} S^{-1}) FOR FOUR TYPES OF GROUND WATER EQUILIBRATED WITH 200 BARS OF CO_2

Microbial Redox Reactions	13. Do 20	14. Do 45	15. Do 80	16. LS 20	17. LS 45	18. LS 80	19. MS 20	20. MS 45	21. MS 80	22. Br 20	23. Br 45	24. Br 80
(1) $H_2 + S \rightarrow HS^- + H^+$	-2.7×10^{-12}	-4.0×10^{-12}	-8.3×10^{-12}	-2.3×10^{-13}	-3.3×10^{-13}	-4.7×10^{-13}	-2.8×10^{-10}	**-8.3×10^{-10}**	-1.2×10^{-09}	-7.1×10^{-10}	**-1.1×10^{-09}**	-2.0×10^{-09}
(2) $3H_2 + N_2 \rightarrow 2NH_3$	-1.4×10^{-12}	-1.9×10^{-12}	-2.6×10^{-12}	-1.2×10^{-13}	-1.7×10^{-13}	-2.1×10^{-13}	-3.5×10^{-10}	**-5.1×10^{-10}**	-7.1×10^{-10}	-9.1×10^{-10}	**-1.4×10^{-09}**	-1.9×10^{-09}
(3) $CH_4 + SO_4^{2-} \rightarrow H_2O + HCO_3^- + HS^-$	**-4.7×10^{-11}**	-7.4×10^{-11}	-1.2×10^{-10}	-8.4×10^{-11}	**-1.3×10^{-10}**	-2.1×10^{-10}	-1.9×10^{-10}	**-3.1×10^{-10}**	-5.0×10^{-10}	-5.3×10^{-10}	**-8.7×10^{-10}**	-1.4×10^{-09}
(4) $4H_2 + H^+ + SO_4^{2-} \rightarrow HS^- + 4H_2O$	-1.0×10^{-12}	-1.4×10^{-12}	-1.8×10^{-12}	-8.2×10^{-14}	-1.1×10^{-13}	-1.3×10^{-13}	-2.7×10^{-10}	**-4.0×10^{-10}**	-5.7×10^{-10}	-7.2×10^{-10}	**-1.1×10^{-09}**	-1.6×10^{-09}
(5) Acetate $+ 4MnO_2 + 7H^+ \rightarrow 4Mn^{2+} + 4H_2O + 2HCO_3^-$	**-5.2×10^{-11}**	-8.0×10^{-11}	-1.2×10^{-10}	-6.8×10^{-11}	**-1.0×10^{-10}**	-1.6×10^{-10}	-1.3×10^{-10}	**-2.0×10^{-10}**	-2.9×10^{-10}	-3.4×10^{-10}	**-5.2×10^{-10}**	-7.9×10^{-10}
(6) $3H_2 + CO \rightarrow CH_4 + H_2O$	-9.0×10^{-13}	-1.2×10^{-12}	-1.4×10^{-12}	-6.9×10^{-14}	-8.4×10^{-14}	-7.7×10^{-14}	-2.5×10^{-10}	**-3.6×10^{-10}**	-4.8×10^{-10}	-6.8×10^{-10}	**-9.9×10^{-10}**	-1.3×10^{-09}
(7) $4H_2 + H^+ + HCO_3^- \rightarrow CH_4 + 3H_2O$	-6.4×10^{-13}	-8.4×10^{-13}	-9.1×10^{-13}	-4.5×10^{-14}	-5.2×10^{-14}	-3.8×10^{-14}	-1.9×10^{-10}	**-2.7×10^{-10}**	-3.5×10^{-10}	-5.1×10^{-10}	**-7.3×10^{-10}**	-9.8×10^{-10}
(8) $4CO + SO_4^{2-} + 4H_2O \rightarrow 4HCO_3^- + HS^- + 3H^+$	-2.0×10^{-13}	-2.9×10^{-13}	-4.0×10^{-13}	-1.4×10^{-13}	-2.1×10^{-13}	-2.9×10^{-13}	-6.0×10^{-12}	-9.1×10^{-12}	-1.3×10^{-11}	-4.7×10^{-11}	-7.1×10^{-11}	-1.0×10^{-10}
(9) $4CO + 5H_2O \rightarrow CH_4 + 3HCO_3^- + 3H^+$	-1.4×10^{-13}	-1.9×10^{-13}	-2.4×10^{-13}	-9.5×10^{-14}	-1.3×10^{-13}	-1.6×10^{-13}	-4.2×10^{-12}	-6.1×10^{-12}	-8.2×10^{-12}	-3.3×10^{-11}	-4.9×10^{-11}	-6.8×10^{-11}
(10) Acetate $+ 4S + 4H_2O \rightarrow 5H^+ + 2HCO_3^- + 4HS^-$	**-1.8×10^{-11}**	-2.9×10^{-11}	-6.6×10^{-11}	-2.0×10^{-11}	**-3.1×10^{-11}**	-4.9×10^{-11}	-9.7×10^{-12}	-6.2×10^{-11}	-9.8×10^{-11}	-2.4×10^{-11}	-4.0×10^{-11}	-1.2×10^{-10}
(11) $CO +$ Hematite $+ 3H^+ \rightarrow 2Fe^{2+} + H_2O + HCO_3^-$	-6.9×10^{-13}	-9.9×10^{-13}	-1.3×10^{-12}	-5.4×10^{-13}	-7.8×10^{-13}	-1.0×10^{-12}	-1.9×10^{-11}	-2.8×10^{-11}	-3.8×10^{-11}	-1.3×10^{-10}	-1.9×10^{-10}	-2.7×10^{-10}
(12) $4H_2 + H^+ + 2HCO_3^- \rightarrow$ Acetate $+ 4H_2O$	-5.5×10^{-13}	-6.8×10^{-13}	-6.3×10^{-13}	-4.0×10^{-14}	-4.2×10^{-14}		-1.8×10^{-10}	**-2.6×10^{-10}**	-3.3×10^{-10}	-4.9×10^{-10}	**-6.9×10^{-10}**	-9.1×10^{-10}
(13) Acetate $+ SO_4^{2-} \rightarrow 2HCO_3^- + HS^-$	-3.8×10^{-12}	-6.2×10^{-12}	-1.0×10^{-11}	-4.5×10^{-12}	-7.3×10^{-12}	-1.2×10^{-11}	-9.7×10^{-12}	-1.6×10^{-11}	-2.6×10^{-11}	-2.6×10^{-11}	-4.2×10^{-11}	-6.9×10^{-11}
(14) $4CO + NO_3^- + 5H_2O \rightarrow 4HCO_3^- + NH_3 + 3H^+$	-8.1×10^{-13}	-1.2×10^{-12}	-1.8×10^{-12}	-5.9×10^{-13}	-9.0×10^{-13}	-1.3×10^{-12}	-2.1×10^{-11}	-3.2×10^{-11}	-4.7×10^{-11}	-1.5×10^{-10}	-2.3×10^{-10}	-3.4×10^{-10}
(15) $2.5CO + NO_3^- + 2H_2O \rightarrow 2.5HCO_3^- + 1.5H^+ + 0.5N_2$	-1.1×10^{-12}	-1.7×10^{-12}	-2.5×10^{-12}	-8.3×10^{-13}	-1.3×10^{-12}	-1.9×10^{-12}	-2.9×10^{-11}	-4.4×10^{-11}	-6.5×10^{-11}	-2.1×10^{-10}	-3.2×10^{-10}	-4.7×10^{-10}
(16) $S_2O_3^{2-} + NO_3^- + 2H_2O \rightarrow 2SO_4^{2-} + H^+ + NH_3$	-2.4×10^{-13}	-3.7×10^{-13}	-4.7×10^{-13}	-5.3×10^{-12}	-8.1×10^{-12}	-1.2×10^{-11}	-2.8×10^{-11}	-4.3×10^{-11}	-6.3×10^{-11}	-1.9×10^{-11}	-2.9×10^{-11}	-4.3×10^{-11}
(17) $4H_2 + NO_3^- + H^+ \rightarrow NH_3 + 3H_2O$	-4.4×10^{-12}	-6.6×10^{-12}	-9.5×10^{-12}	-4.1×10^{-13}	-6.2×10^{-13}	-8.8×10^{-13}	-9.4×10^{-10}	**-1.4×10^{-09}**	-2.1×10^{-09}	-2.4×10^{-09}	**-3.6×10^{-09}**	-5.3×10^{-09}
(18) Acetate $+ NO_3^- + H_2O \rightarrow 2HCO_3^- + NH_3$	**-3.3×10^{-11}**	-5.1×10^{-11}	-7.6×10^{-11}	-5.3×10^{-12}	-8.1×10^{-12}	-1.2×10^{-11}	-2.6×10^{-11}	-4.0×10^{-11}	-6.0×10^{-11}	-1.7×10^{-11}	-2.7×10^{-11}	-4.0×10^{-11}
(19) $5H_2 + 2NO_3^- + 2H^+ \rightarrow N_2 + 6H_2O$	-6.2×10^{-12}	-9.3×10^{-12}	-1.4×10^{-11}	-5.3×10^{-12}	-8.1×10^{-12}	-1.2×10^{-11}	-2.6×10^{-11}	-3.8×10^{-11}	-5.6×10^{-11}	-1.9×10^{-11}	-2.8×10^{-11}	-4.2×10^{-11}
(20) $2S + 1.5NO_3^- + 3.5H_2O \rightarrow 2SO_4^{2-} + 2.5H^+ + 1.5NH_3$	**-7.0×10^{-11}**	-1.1×10^{-10}	-1.6×10^{-10}	-4.6×10^{-12}	-7.0×10^{-12}	-1.1×10^{-11}	-2.3×10^{-11}	-3.5×10^{-11}	-5.3×10^{-11}	-1.5×10^{-11}	-2.3×10^{-11}	-3.5×10^{-11}
(21) Acetate $+ 1.6NO_3^- + 0.6H^+ \rightarrow 2HCO_3^- + 0.8H_2O + 0.8N_2$	**-4.8×10^{-11}**	-7.4×10^{-11}	-1.1×10^{-10}	-4.9×10^{-12}	-7.5×10^{-12}	-1.1×10^{-11}	-2.4×10^{-11}	-3.7×10^{-11}	-5.5×10^{-11}	-1.6×10^{-11}	-2.5×10^{-11}	-3.7×10^{-11}
(22) $HS^- + NO_3^- + H_2O \rightarrow SO_4^{2-} + NH_3$	**-7.0×10^{-11}**	-1.1×10^{-10}	-1.6×10^{-10}	-4.6×10^{-12}	-7.0×10^{-12}	-1.0×10^{-11}	-2.3×10^{-11}	-3.5×10^{-11}	-5.2×10^{-11}	-1.5×10^{-11}	-2.3×10^{-11}	-3.5×10^{-11}
(23) $CO + 2H_2O \rightarrow HCO_3^- + H^+ + H_2$												
(24) Acetate $+ H_2O \rightarrow CH_4 + HCO_3^-$												
(25) $NO_2^- + H^+ + NH_3 \rightarrow 2H_2O + N_2$	-5.5×10^{-13}	-8.4×10^{-13}	-1.2×10^{-12}	-3.2×10^{-13}	-4.9×10^{-13}	-7.3×10^{-13}	-2.2×10^{-12}	-3.4×10^{-12}	-5.0×10^{-12}	-5.5×10^{-12}	-8.4×10^{-12}	-1.3×10^{-11}

(26) $S_2O_3^{2-} + 4H_2 \rightarrow 3H_2O + 2HS^-$	-7.4×10^{-14}	-1.0×10^{-13}	-4.6×10^{-14}	-9.7×10^{-14}	-1.4×10^{-13}	-1.7×10^{-13}	-3.1×10^{-10}	**-4.6×10^{-10}**	-6.6×10^{-10}	-7.9×10^{-10}	**-1.2×10^{-09}**	-1.7×10^{-09}
(27) 4Formate $+ H^+ + H_2O \rightarrow CH_4 + 3HCO_3^-$	-8.4×10^{-12}	-1.2×10^{-11}	-1.7×10^{-11}	-2.5×10^{-13}	-3.2×10^{-13}	-3.6×10^{-13}	-5.3×10^{-13}	-7.1×10^{-13}	-8.3×10^{-13}	-3.3×10^{-12}	-4.7×10^{-12}	-6.1×10^{-12}
(28) $5Fe^{2+} + NO_3^- + 12H_2O \rightarrow 5Fe(OH)_3 + 9H^+ + 0.5N_2$		-1.1×10^{-12}	-2.3×10^{-12}		-4.6×10^{-13}	-1.1×10^{-12}		-6.9×10^{-13}	-1.6×10^{-12}		-3.5×10^{-12}	-3.8×10^{-12}
(29) $S_2O_3^{2-} + H_2O \rightarrow SO_4^{2-} + H^+ + HS^-$				-4.2×10^{-15}	-6.8×10^{-15}	-1.1×10^{-14}	-1.2×10^{-12}	-1.9×10^{-12}	-3.2×10^{-12}	-7.5×10^{-13}	-1.2×10^{-12}	-2.0×10^{-12}
(30) Acetate + 4Hematite $+ 15H^+ \rightarrow 8Fe^{2+} + 8H_2O + 2HCO_3^-$	**-2.7×10^{-11}**	-4.0×10^{-11}	-5.3×10^{-11}	-3.6×10^{-11}	**-5.3×10^{-11}**	-7.2×10^{-11}	-7.3×10^{-11}	-1.1×10^{-10}	-1.5×10^{-10}	-1.7×10^{-10}	-2.5×10^{-10}	-3.5×10^{-10}
(31) H_2 + Hematite $+ 4H^+ \rightarrow 2Fe^{2+} + 3H_2O$	**-1.3×10^{-11}**	-1.8×10^{-11}	-2.5×10^{-11}	-1.3×10^{-12}	-2.0×10^{-12}	-2.7×10^{-12}	-2.7×10^{-09}	**-4.0×10^{-09}**	-5.5×10^{-09}	-6.4×10^{-09}	**-9.3×10^{-09}**	-1.3×10^{-08}
(32) Propionate $+ 3H_2O \rightarrow$ Acetate $+ HCO_3^- + H^+ + 3H_2$												
(33) $2CO + O_2 + 2H_2O \rightarrow 2HCO_3^- + 2H^+$	-2.6×10^{-56}	-4.0×10^{-52}	-8.1×10^{-36}	-2.3×10^{-59}	-1.1×10^{-54}	-5.2×10^{-49}	-1.4×10^{-74}	-3.9×10^{-55}	-5.8×10^{-51}	-1.4×10^{-77}	-2.1×10^{-70}	-4.0×10^{-59}
(34) $2H_2 + O_2 \rightarrow 2H_2O$	-2.5×10^{-56}	-3.7×10^{-52}	-7.7×10^{-36}	-2.1×10^{-59}	-9.4×10^{-55}	-4.4×10^{-49}	-1.4×10^{-74}	-3.9×10^{-55}	-5.8×10^{-51}	-1.3×10^{-77}	-2.0×10^{-70}	-3.8×10^{-59}
(35) Acetate $+ 2O_2 \rightarrow 2HCO_3^- + H^+$	-2.0×10^{-56}	-3.1×10^{-52}	-7.1×10^{-36}	-1.7×10^{-59}	-8.2×10^{-55}	-4.2×10^{-49}	-5.8×10^{-75}	-2.7×10^{-55}	-4.3×10^{-51}	-4.2×10^{-78}	-6.9×10^{-71}	-2.1×10^{-59}
(36) $CH_4 + 2O_2 \rightarrow HCO_3^- + H^+ + H_2O$	-1.9×10^{-56}	-3.0×10^{-52}	-6.9×10^{-36}	-1.7×10^{-59}	-7.9×10^{-55}	-4.1×10^{-49}	-5.5×10^{-75}	-2.6×10^{-55}	-4.1×10^{-51}	-3.8×10^{-78}	-6.2×10^{-71}	-2.0×10^{-59}
(37) $S + 1.5O_2 + H_2O \rightarrow SO_4^{2-} + 2H^+$	-1.6×10^{-62}			-1.3×10^{-59}	-6.3×10^{-55}	-3.3×10^{-49}		-2.0×10^{-55}	-3.2×10^{-51}			-3.4×10^{-60}
(38) $S_2O_3^{2-} + 2O_2 + H_2O \rightarrow 2SO_4^{2-} + 2H^+$	-1.6×10^{-56}	-2.5×10^{-52}	-5.0×10^{-36}	-1.5×10^{-59}	-7.0×10^{-55}	-3.6×10^{-49}	-3.2×10^{-75}	-2.3×10^{-55}	-3.5×10^{-51}	-1.1×10^{-78}	-1.7×10^{-71}	-1.3×10^{-59}
(39) $HS^- + 2O_2 \rightarrow SO_4^{2-} + H^+$	-1.6×10^{-56}	-2.4×10^{-52}	-6.0×10^{-36}	-1.4×10^{-59}	-6.3×10^{-55}	-3.2×10^{-49}	-1.6×10^{-75}	-2.0×10^{-55}	-3.1×10^{-51}			-9.1×10^{-60}
(40) $2HS^- + 2O_2 \rightarrow S_2O_3^{2-} + H_2O$	-1.5×10^{-56}	-2.4×10^{-52}	-7.1×10^{-36}	-1.2×10^{-59}	-5.6×10^{-55}	-2.8×10^{-49}		-1.7×10^{-55}	-2.7×10^{-51}			-5.6×10^{-60}
(41) $2HS^- + O_2 + 2H^+ \rightarrow 2S + 2H_2O$	-1.6×10^{-56}	-2.4×10^{-52}	-5.7×10^{-36}	-1.4×10^{-59}	-6.4×10^{-55}	-3.0×10^{-49}	-2.4×10^{-75}	-2.0×10^{-55}	-2.9×10^{-51}			-7.4×10^{-60}
(42) HS^- + 4Hematite $+ 15H^+ \rightarrow SO_4^{2-} + 8Fe^{2+} + 8H_2O$	**-8.2×10^{-10}**	-1.2×10^{-09}	-1.5×10^{-09}	-2.9×10^{-09}	**-4.2×10^{-09}**	-5.6×10^{-09}	-1.8×10^{-09}	**-2.7×10^{-09}**	-3.5×10^{-09}	-2.0×10^{-09}	**-2.9×10^{-09}**	-3.9×10^{-09}
(43) $4Fe^{2+} + O_2 + 10H_2O \rightarrow 4Fe(OH)_3 + 8H^+$												

Microbial redox reactions have been ordered according to their power with the most powerful reactions for the 80 °C brine appearing first. The microbial reaction numbers and column heading numbers refer to Figure 3. The power is not reported for reactions for which the free energy was > -20 kJ mol^{-1}. The values in bold represent the top 10 values.

The free energies of the nitrate reduction reactions were greater with the N_2 producing reactions being more favored than before. In terms of the potential microbial power values, the hematite reduction reaction by oxidation of HS^- (reaction (42) in Table 6) became the most powerful suggesting that this abiotic reaction will dominate in siliclastic aquifers where Fe(III) oxides and HS^- are present and will significantly ameliorate the low pH conditions. In the more saline aquifers where H_2 are high, the microbial reduction of Fe(III) oxides are equally important and will dominate if HS^- is limiting. These reactions will also raise the pH of the ground water and promote precipitation of the CO_2 as carbonate.

In terms of the available microbial power for the top 10 reactions, the CO_2 injection has increased power levels by a factor of 10. This is primarily the result of the reduction in pH. For many of the microorganisms, this pH range falls below their optimal growth regime so that the increased power may not be immediately available until the pH increases. Initially after CO_2 injection, therefore, an increase of the pH is anticipated due to abiotic redox reactions, such as redox reaction (42) in Table 6, or alteration of the aquifer minerals by the carbonic acid.

Dissolution of Aquifer Minerals

The low pH, CO_2 saturated, dolomitic ground water was reacted with dolomite and calcite to simulate a carbonate aquifer. The low pH, CO_2 saturated, low, moderate and highly saline ground water was reacted with albite and minor calcite to simulate a siliclastic aquifer [23]. The impacts on ground water chemistry were as follows:

1. For the dolomite system, the pH increased from 3.1 to 4.6, the pe decreased from 9.5 to 7.5 and the dissolved CO_2 decreased slightly from 7.99 to 7.91 M. As dolomite and calcite dissolved, chalcedony, kaolinite, hydroxyapatite, fluorite and various metal sulfide minerals precipitated until dolomite and subsequently calcite attained saturation. The reaction led to a net increase in porosity of 0.3%. The only significant difference in simulations at higher aquifer temperatures is that more carbonate precipitation occurred with no significant change in the porosity.
2. For the low salinity ground water, the pH increased from 2.9 to 7, the pe decreased from 5.7 to -2.8 and the dissolved CO_2 decreased from 7.99 to 0.2 M. In terms of pH and pe, these values are close to that of the initial ground water (Table 2). As albite and calcite dissolved, chalcedony, kaolinite and nahcolite, the Na bicarbonate mineral species, and minor sulfide mineral phases precipitated. The reaction led to a 20% reduction in porosity. For 80 °C, the reaction increased the pH to 6, decreased the pe to -1.9 and reduced the dissolved CO_2 to 1.3 M with no significant change in the porosity primarily because nahcolite did not precipitate.
3. For the moderate salinity ground water, the pH increased from 2.9 to 7, the pe decreased from 2 to -3.4 and the dissolved CO_2 decreased slightly from 7.99 to 0.2 M. In terms of pH and pe, these values are close to that of the initial ground water (Table 2). As albite and calcite dissolved, chalcedony, kaolinite, rhodochrosite and nahcolite and minor sulfide mineral phases precipitated. The reaction led to a 20% reduction in porosity. For 80 °C, the reaction increased the pH to 6, decreased the pe to -1.8 and reduced the dissolved CO_2 to 1.3 M with no significant change in the porosity primarily because nahcolite did not precipitate.
4. For the high salinity ground water, the pH increased from 2.7 to 6.9, the pe decreased from 2 to -3.3 and the dissolved CO_2 decreased slightly from 7.99 to 0.2 M. In terms of pH and pe, these values are close to that of the initial ground water (Table 2). As albite and calcite dissolved, chalcedony, kaolinite, rhodochrosite, dolomite, witherite and nahcolite and minor sulfide mineral phases precipitated. The reaction led to a 20% reduction in porosity. For 80 °C, the reaction increased the pH to 6, decreased the pe to -1.8 and reduced the dissolved CO_2 to 1.3 M with a 0.3% increase in the porosity primarily because nahcolite and the other carbonate minerals did not precipitate, although minor siderite did.

With the dissolution reactions ameliorating some of the effects of CO_2 injection, the only significant change in the microbial redox reactions were the following:

1. The fermentation reactions of acetate fermentation to CH_4 and CO_2 (reaction (36) in Table 7) and propionate fermentation to acetate, CO_2 and H_2 (reaction (42) in Table 7) still remain unfavorable for any of the ground water compositions. This would be a serious impediment to strictly aceticlastic

TABLE 7

FREE ENERGY (KJ MOL^{-1}) OF REDOX REACTIONS AFTER INTERACTION OF CO_2 SATURATED WATER WITH AQUIFER MINERALS

Microbial Redox Reactions	25. Do 20	26. Do 45	27. Do 80	28. LS 20	29. LS 45	30. LS 80	31. MS 20	32. MS 45	33. MS 80	34. Br 20	35. Br 45	36. Br 80
(1) $5H_2 + 2NO_3^- + 2H^+ \rightarrow N_2 + 6H_2O$	−1224	−1103	−961	−1140	−1023	−885	−1252	−1135	−997	−1268	−1151	−1013
(2) Acetate + $1.6NO_3^- + 0.6H^+ \rightarrow$ $2HCO_3^- + 0.8H_2O + 0.8N_2$	−888	−816	−732	−849	−773	−690	−856	−781	−697	−860	−783	−700
(3) $2S + 1.5NO_3^- + 3.5H_2O \rightarrow$ $2SO_4^{2-} + 2.5H^+ + 1.5NH_3$				−835	−765	−683	−833	−763	−680	−824	−754	−671
(4) $4CO + NO_3^- + 5H_2O \rightarrow$ $4HCO_3^- + NH_3 + 3H^+$	−705	−636	−555	−702	−614	−525	−744	−657	−567	−766	−679	−589
(5) Acetate + $4MnO_2 + 7H^+ \rightarrow$ $4Mn^{2+} + 4H_2O + 2HCO_3^-$	−907	−831	−741	−812	−764	−691	−797	−739	−662	−799	−742	−671
(6) $2.5CO + NO_3^- + 2H_2O \rightarrow$ $2.5HCO_3^- + 1.5H^+ + 0.5N_2$	−624	−565	−496	−622	−550	−476	−651	−579	−505	−664	−593	−518
(7) $4H_2 + NO_3^- + H^+ \rightarrow NH_3 + 3H_2O$	−686	−614	−530	−618	−552	−471	−705	−639	−557	−718	−651	−570
(8) Acetate + $NO_3^- + H_2O \rightarrow$ $2HCO_3^- + NH_3$	−595	−547	−493	−556	−507	−453	−560	−511	−457	−563	−513	−460
(9) $S_2O_3^{2-} + NO_3^- + 2H_2O \rightarrow$ $2SO_4^{2-} + H^+ + NH_3$	−485	−446	−388	−567	−519	−460	−566	−518	−459	−558	−509	−451
(10) $HS^- + NO_3^- + H_2O \rightarrow$ $SO_4^{2-} + NH_3$	−548	−499	−443	−540	−493	−436	−538	−491	−434	−534	−488	−430
(11) Acetate + $2O_2 \rightarrow 2HCO_3^- + H^+$	−483	−440	−415	−65	−64	−75	−36	−72	−83	−43	−39	−40
(12) Acetate + $4S + 4H_2O \rightarrow$ $5H^+ + 2HCO_3^- + 4HS^-$				−65	−64	−75	−28	−72	−83	−37	−32	−31
(13) $5Fe^{2+} + NO_3^- + 12H_2O \rightarrow$ $5Fe(OH)_3 + 9H^+ + 0.5N_2$	−132	−129	−127	−214	−186	−160	−168	−189	−163	−175	−188	−162
(14) $NO_2^- + H^+ + NH_3 \rightarrow 2H_2O + N_2$	−356	−324	−286	−349	−316	−280	−358	−325	−288	−359	−326	−289
(15) $CH_4 + 2O_2 \rightarrow$ $HCO_3^- + H^+ + H_2O$	−470	−426	−400	−62	−63	−73	−36	−74	−83	−43	−40	−40
(16) $S_2O_3^{2-} + 2O_2 + H_2O \rightarrow$ $2SO_4^{2-} + 2H^+$	−373	−339	−310	−77	−76	−82	−43	−79	−85	−39	−35	−31
(17) $HS^- + 2O_2 \rightarrow SO_4^{2-} + H^+$	−436	−392	−365	−49	−50	−58	−15	−52	−59	*− 15*	*− 13*	*− 11*
(18) $2HS^- + 2O_2 \rightarrow S_2O_3^{2-} + H_2O$	−499	−445	−420	−22	−25	−33	14	−26	−34	*8*	*8*	*10*
(19) $2CO + O_2 + 2H_2O \rightarrow$ $2HCO_3^- + 2H^+$	−296	−264	−238	−105	−86	−73	−110	−109	−97	−123	−102	−85

(*continued*)

TABLE 7
CONTINUED

Microbial Redox Reactions	25. Do 20	26. Do 45	27. Do 80	28. LS 20	29. LS 45	30. LS 80	31. MS 20	32. MS 45	33. MS 80	34. Br 20	35. Br 45	36. Br 80
(20) $4CO + SO_4^{2-} + 4H_2O \rightarrow 4HCO_3^- + HS^- + 3H^+$	−156	−137	−112	−161	−121	−89	−206	−166	−134	−232	−191	−159
(21) $S + 1.5O_2 + H_2O \rightarrow SO_4^{2-} + 2H^+$							*−18*			*−18*	*−16*	*−14*
(22) $4CO + 5H_2O \rightarrow CH_4 + 3HCO_3^- + 3H^+$	−123	−103	−77	−149	−108	−74	−184	−144	−110	−204	−164	−130
(23) $2H_2 + O_2 \rightarrow 2H_2O$	−287	−253	−226	−64	−55	−46	−91	−100	−92	−99	−88	−75
(24) $S_2O_3^{2-} + 4H_2 \rightarrow 3H_2O + 2HS^-$	−75	−61	−32	−105	−84	−60	−195	−174	−149	−207	−185	−160
(25) $2HS^- + O_2 + 2H^+ \rightarrow 2S + 2H_2O$	−210	−183	−163	0	0	0	*18*	*0*	*0*	*15*	*16*	*21*
(26) $H_2 + S \rightarrow HS^- + H^+$				−32	−27	−23	−43	−50	−46	−48	−42	−35
(27) $3H_2 + CO \rightarrow CH_4 + H_2O$	−109	−86	−58	−86	−61	−33	−155	−130	−102	−168	−144	−115
(28) $4H_2 + H^+ + SO_4^{2-} \rightarrow HS^- + 4H_2O$	−138	−114	−87	−78	−59	−35	−167	−148	−124	−183	−163	−140
(29) $3H_2 + N_2 \rightarrow 2NH_3$	−148	−125	−100	−96	−81	−57	−158	−142	−118	−167	−151	−127
(30) $4Formate + H^+ + H_2O \rightarrow CH_4 + 3HCO_3^-$	−73	−63	−52	*2*	*19*	*28*	*−2*	*14*	*24*	*−21*	*−4*	*6*
(31) $Acetate + SO_4^{2-} \rightarrow 2HCO_3^- + HS^-$	−46	−48	−50	−15	−14	−17	−22	−20	−24	−28	−26	−30
(32) $4H_2 + H^+ + HCO_3^- \rightarrow CH_4 + 3H_2O$	−104	−81	−52	−65	−46	−20	−145	−126	−100	−156	−137	−111
(33) $CO + Hematite + 3H^+ \rightarrow 2Fe^{2+} + H_2O + HCO_3^-$	−120	−102	−78	−87	−73	−58	−94	−83	−68	−101	−89	−73
(34) $CO + 2H_2O \rightarrow HCO_3^- + H^+ + H_2$	*−5*	*−6*	*−6*	*−21*	*−16*	*−14*	*−10*	*−5*	*−2*	*−12*	*−7*	*−5*

(35) $CH_4 + SO_4^{2-} \rightarrow H_2O + HCO_3^- + HS^-$	−33	−34	−35	−13	−13	−15	−22	−22	−24	−27	−27	−29
(36) Acetate $+ H_2O \rightarrow CH_4 + HCO_3^-$	*−13*	*−14*	*−15*	*−2*	*−1*	*−2*	*0*	*2*	*1*	*−1*	*1*	*0*
(37) $4H_2 + H^+ + 2HCO_3^- \rightarrow$ Acetate $+ 4H_2O$	−91	−67	−37	−62	−45	−18	−145	−128	−100	−155	−138	−110
(38) $S_2O_3^{2-} + H_2O \rightarrow SO_4^{2-} + H^+ + HS^-$	*63*	*53*	*55*	−27	−26	−24	−28	−27	−26	−23	−21	−20
(39) Acetate + 4Hematite + $15H^+ 8Fe^{2+} + 8H_2O + 2HCO_3^-$	−371	−318	−252	−202	−185	−158	−193	−187	−160	−199	−190	−164
(40) $4Fe^{2+} + O_2 + 10H_2O \rightarrow 4Fe(OH)_3 + 8H^+$	*97*	*85*	*56*				*280*			*271*	*225*	*205*
(41) H_2 + Hematite $+ 4H^+ \rightarrow 2Fe^{2+} + 3H_2O$	−116	−96	−72	−66	−57	−44	−84	−79	−65	−89	−82	−68
(42) Propionate $+ 3H_2O \rightarrow$ Acetate $+ HCO_3^- + H^+ + 3H_2$	*60*	*42*	*20*	*30*	*16*	*−3*	*93*	*80*	*60*	*100*	*86*	*66*
(43) $HS^- + 4$Hematite $+ 15H^+ \rightarrow SO_4^{2-} + 8Fe^{2+} + 8H_2O$	−325	−270	−202	−186	−171	−141	−171	−167	−137	−171	−164	−134
(44) $NH_3 + 1.5{*}O_2 \rightarrow NO_2^- + H^+ + H_2O$	*73*	*68*	*46*	*351*	*316*	*267*	*379*	*317*	*268*	*377*	*344*	*303*
(45) $4Mn^{2+} + NO_3^- + 5H_2O \rightarrow 4MnO_2 + 7H^+ + NH_3$	*313*	*284*	*248*	*256*	*256*	*238*	*237*	*229*	*205*	*237*	*229*	*212*
(46) $2NO_2^- + O_2 \rightarrow 2NO_3^-$	*78*	*77*	*64*	*281*	*255*	*222*	*288*	*244*	*212*	*284*	*260*	*233*
(47) $2Mn^{2+} + O_2 + 2H_2O \rightarrow 2MnO_2 + 4H^+$	*212*	*196*	*163*				*384*			*381*	*355*	*320*

The reactions are ordered from most negative to positive with respect to the free energy for the dolomite ground water at 20 °C. The microbial reaction numbers and column heading numbers refer to Figure 10. Values in italics are > -20 kJ mol^{-1} and therefore are not considered to be viable for microbial metabolism.

TABLE 8
POTENTIAL MICROBIAL POWER (5000 KJ CELL^{-1} S^{-1}) AFTER INTERACTION OF CO_2 SATURATED WATER WITH AQUIFER MINERALS

Microbial Redox Reactions	25. Do 20	26. Do 45	27. Do 80	28. LS 20	29. LS 45	30. LS 80	31. MS 20	32. MS 45	33. MS 80	34. Br 20	35. Br 45	36. Br 80
(1) $H_2 + S \rightarrow HS^- + H^+$				-1.6×10^{-13}	-2.3×10^{-13}	-3.2×10^{-13}	-2.1×10^{-10}	**-4.1×10^{-10}**	-6.4×10^{-10}	-8.3×10^{-10}	**-7.0×10^{-10}**	-1.2×10^{-09}
(2) $3H_2 + N_2 \rightarrow 2NH_3$	-1.2×10^{-12}	-1.7×10^{-12}	-2.3×10^{-12}	-1.6×10^{-13}	-2.2×10^{-13}	-2.6×10^{-13}	-2.6×10^{-10}	**-3.9×10^{-10}**	-5.5×10^{-10}	-9.6×10^{-10}	**-8.4×10^{-10}**	-1.5×10^{-09}
(3) $CH_4 + SO_4^{2-} \rightarrow H_2O + HCO_3^- + HS^-$	**-2.7×10^{-11}**	-4.7×10^{-11}	-8.1×10^{-11}				-8.3×10^{-10}	**-1.4×10^{-09}**	-2.6×10^{-09}	-5.2×10^{-10}	**-4.3×10^{-10}**	-7.9×10^{-10}
(4) $4H_2 + H^+ + SO_4^{2-} \rightarrow HS^- + 4H_2O$	-8.5×10^{-13}	-1.2×10^{-12}	-1.5×10^{-12}	-9.6×10^{-14}	-1.2×10^{-13}	-1.2×10^{-13}	-2.1×10^{-10}	**-3.1×10^{-10}**	-4.3×10^{-10}	-7.9×10^{-10}	**-6.8×10^{-10}**	-1.2×10^{-09}
(5) Acetate + $4MnO_2 + 7H^+ \rightarrow 4Mn^{2+} + 4H_2O + 2HCO_3^-$	**-3.0×10^{-11}**	-4.6×10^{-11}	-7.0×10^{-11}	-5.4×10^{-11}	**-8.5×10^{-11}**	-1.3×10^{-10}	-1.1×10^{-10}	**-1.7×10^{-10}**	-2.5×10^{-10}	-1.6×10^{-10}	-2.5×10^{-10}	-3.8×10^{-10}
(6) $3H_2 + CO \rightarrow CH_4 + H_2O$	-9.0×10^{-13}	-1.2×10^{-12}	-1.4×10^{-12}	-1.4×10^{-13}	-1.7×10^{-13}	-1.6×10^{-13}	-2.5×10^{-10}	**-3.6×10^{-10}**	-4.8×10^{-10}	-9.7×10^{-10}	**-8.0×10^{-10}**	-1.3×10^{-09}
(7) $4H_2 + H^+ + HCO_3^- \rightarrow CH_4 + 3H_2O$	-6.4×10^{-13}	-8.4×10^{-13}	-9.1×10^{-13}	-8.0×10^{-14}	-9.5×10^{-14}	-6.9×10^{-14}	-1.8×10^{-10}	**-2.6×10^{-10}**	-3.5×10^{-10}	-6.7×10^{-10}	**-5.7×10^{-10}**	-9.7×10^{-10}
(8) $4CO + SO_4^{2-} + 4H_2O \rightarrow 4HCO_3^- + HS- + 3H^+$	-1.7×10^{-13}	-2.6×10^{-13}	-3.5×10^{-13}	-1.8×10^{-13}	-2.3×10^{-13}	-2.8×10^{-13}	-1.1×10^{-11}	-1.6×10^{-11}	-2.1×10^{-11}	-5.8×10^{-11}	-7.2×10^{-11}	-1.0×10^{-10}
(9) $4CO + 5H_2O \rightarrow CH_4 + 3HCO_3^- + 3H^+$	-1.4×10^{-13}	-1.9×10^{-13}	-2.4×10^{-13}	-1.7×10^{-13}	-2.0×10^{-13}	-2.3×10^{-13}	-1.0×10^{-11}	-1.3×10^{-11}	-1.7×10^{-11}	-5.1×10^{-11}	-6.1×10^{-11}	-8.2×10^{-11}
(10) Acetate + 4S + $4H_2O \rightarrow 5H^+ + 2HCO_3^- + 4HS^-$				-4.3×10^{-12}	**-7.2×10^{-12}**	-1.4×10^{-11}	-3.7×10^{-12}	-1.6×10^{-11}	-3.1×10^{-11}	-7.3×10^{-12}	-1.1×10^{-11}	-1.8×10^{-11}
(11) CO + Hematite + $3H^+ \rightarrow 2Fe^{2+} + H_2O + HCO_3^-$	-5.4×10^{-13}	-7.6×10^{-13}	-9.9×10^{-13}	-3.9×10^{-13}	-5.5×10^{-13}	-7.2×10^{-13}	-2.1×10^{-11}	-3.1×10^{-11}	-4.3×10^{-11}	-1.0×10^{-10}	-1.3×10^{-10}	-1.8×10^{-10}
(12) $4H_2 + H^+ + 2HCO_3^- \rightarrow$ Acetate + $4H_2O$	-5.6×10^{-13}	-6.9×10^{-13}	-6.5×10^{-13}	-7.7×10^{-14}	-9.3×10^{-14}		-1.8×10^{-10}	**-2.7×10^{-10}**	-3.5×10^{-10}	-6.7×10^{-10}	**-5.7×10^{-10}**	-9.6×10^{-10}
(13) Acetate + $SO_4^{2-} \rightarrow 2HCO_3^- + HS^-$	-1.5×10^{-12}	-2.7×10^{-12}	-4.7×10^{-12}	-1.0×10^{-12}	-1.5×10^{-12}	-3.3×10^{-12}	-2.9×10^{-12}	-4.4×10^{-12}	-8.8×10^{-12}	-5.6×10^{-12}	-8.6×10^{-12}	-1.7×10^{-11}
(14) $4CO + NO_3^- + 5H_2O \rightarrow 4HCO_3^- + NH_3 + 3H^+$	-7.9×10^{-13}	-1.2×10^{-12}	-1.7×10^{-12}	-7.8×10^{-13}	-1.2×10^{-12}	-1.7×10^{-12}	-4.1×10^{-11}	-6.2×10^{-11}	-8.9×10^{-11}	-1.9×10^{-10}	-2.5×10^{-10}	-3.7×10^{-10}
(15) $2.5CO + NO_3^- + 2H_2O \rightarrow 2.5HCO_3^- + 1.5H^+ + 0.5N_2$	-1.1×10^{-12}	-1.7×10^{-12}	-2.5×10^{-12}	-1.1×10^{-12}	-1.7×10^{-12}	-2.4×10^{-12}	-5.8×10^{-11}	-8.7×10^{-11}	-1.3×10^{-10}	-2.7×10^{-10}	-3.6×10^{-10}	-5.2×10^{-10}
(16) $S_2O_3^{2-} + NO_3^- + 2H_2O \rightarrow 2SO_4^{2-} + H^+ + NH_3$	-2.7×10^{-13}	-4.1×10^{-13}	-6.0×10^{-13}	-7.1×10^{-12}	**-1.1×10^{-11}**	-1.5×10^{-11}	-2.8×10^{-11}	-4.2×10^{-11}	-6.1×10^{-11}	-1.9×10^{-11}	-2.8×10^{-11}	-4.2×10^{-11}
(17) $4H_2 + NO_3^- + H^+ \rightarrow NH_3 + 3H_2O$	-4.2×10^{-12}	-6.4×10^{-12}	-9.3×10^{-12}	-7.6×10^{-13}	-1.1×10^{-12}	-1.6×10^{-12}	-8.7×10^{-10}	**-1.3×10^{-09}**	-1.9×10^{-09}	-3.1×10^{-09}	**-2.7×10^{-09}**	-5.0×10^{-09}
(18) Acetate + $NO_3^- + H_2O \rightarrow 2HCO_3^- + NH_3$	**-2.0×10^{-11}**	-3.1×10^{-11}	-4.6×10^{-11}	-6.8×10^{-12}	**-1.0×10^{-11}**	-1.6×10^{-11}	-2.4×10^{-11}	-3.7×10^{-11}	-5.5×10^{-11}	-1.6×10^{-11}	-2.5×10^{-11}	-3.7×10^{-11}
(19) $5H_2 + 2NO_3^- + 2H^+ \rightarrow N_2 + 6H_2O$	**-6.1×10^{-12}**	-9.2×10^{-12}	-1.3×10^{-11}	-7.0×10^{-12}	**-1.1×10^{-11}**	-1.6×10^{-11}	-2.4×10^{-11}	-3.7×10^{-11}	-5.4×10^{-11}	-1.8×10^{-11}	-2.7×10^{-11}	-4.0×10^{-11}
(20) $2S + 1.5NO_3^- + 3.5H_2O \rightarrow 2SO_4^{2-} + 2.5H^+ + 1.5NH_3$				-6.4×10^{-12}	**-9.8×10^{-12}**	-1.5×10^{-11}	-2.4×10^{-11}	-3.7×10^{-11}	-5.5×10^{-11}	-1.6×10^{-11}	-2.4×10^{-11}	-3.6×10^{-11}
(21) Acetate + $1.6NO_3^- + 0.6H^+ \rightarrow 2HCO_3^- + 0.8H_2O + 0.8N_2$	**-3.0×10^{-11}**	-4.6×10^{-11}	-6.9×10^{-11}	-6.3×10^{-12}	**-9.8×10^{-12}**	-1.5×10^{-11}	-2.3×10^{-11}	-3.5×10^{-11}	-5.2×10^{-11}	-1.5×10^{-11}	-2.3×10^{-11}	-3.5×10^{-11}
(22) $HS^- + NO_3^- + H_2O \rightarrow SO_4^{2-} + NH_3$	**-7.0×10^{-11}**	-1.1×10^{-10}	-1.6×10^{-10}	-6.2×10^{-12}	**-9.5×10^{-12}**	-1.4×10^{-11}	-2.3×10^{-11}	-3.5×10^{-11}	-5.2×10^{-11}	-1.5×10^{-11}	-2.3×10^{-11}	-3.5×10^{-11}
(23) $CO + 2H_2O \rightarrow HCO_3^- + H^+ + H_2$			-1.9×10^{-14}									
(24) Acetate + $H_2O \rightarrow CH_4 + HCO_3^-$												
(25) $NO_2^- + H^+ + NH_3 \rightarrow 2H_2O + N_2$	-1.1×10^{-12}	-1.7×10^{-12}	-2.5×10^{-12}	-5.4×10^{-13}	-8.2×10^{-13}	-1.2×10^{-12}	-5.5×10^{-12}	-8.4×10^{-12}	-1.3×10^{-11}	-1.1×10^{-11}	-1.7×10^{-11}	-2.5×10^{-11}

(26) $S_2O_3^{2-} + 4H_2 \rightarrow 3H_2O + 2HS^-$	-4.1×10^{-14}	-5.6×10^{-14}	-5.0×10^{-14}	-1.3×10^{-13}	-1.8×10^{-13}	-2.1×10^{-13}	-2.4×10^{-10}	-3.6×10^{-10}	-5.2×10^{-10}	-8.9×10^{-10}	$\mathbf{-7.7 \times 10^{-10}}$	-1.4×10^{-09}
(27) $4Formate + H^+ + H_2O \rightarrow CH_4 + 3HCO_3^-$	-4.5×10^{-12}	-6.5×10^{-12}	-9.0×10^{-12}							8.8×10^{-14}		
(28) $5Fe^{2+} + NO_3^- + 12H_2O \rightarrow 5Fe(OH)_3 + 9H^+ + 0.5N_2$		-2.9×10^{-12}	-4.7×10^{-12}		-1.4×10^{-13}	-2.0×10^{-13}		-3.5×10^{-13}	-5.1×10^{-13}		-7.0×10^{-13}	
(29) $S_2O_3^{2-} + H_2O \rightarrow SO_4^{2-} + H^+ + HS^-$				-7.5×10^{-13}	$\mathbf{-1.2 \times 10^{-12}}$	-1.9×10^{-12}	-1.6×10^{-12}	-2.5×10^{-12}	-4.0×10^{-12}	-9.0×10^{-13}	-1.4×10^{-12}	-2.2×10^{-12}
(30) $Acetate + 4Hematite + 15H^+ \rightarrow 8Fe^{2+} + 8H_2O + 2HCO_3^-$	$\mathbf{-1.2 \times 10^{-11}}$	-1.8×10^{-11}	-2.4×10^{-11}	-1.3×10^{-11}	-2.1×10^{-11}	-3.0×10^{-11}	-2.6×10^{-11}	-4.2×10^{-11}	-6.0×10^{-11}	-4.0×10^{-11}	-6.4×10^{-11}	-9.2×10^{-11}
(31) $H_2 + Hematite + 4H^+ \rightarrow 2Fe^{2+} + 3H_2O$	$\mathbf{-9.2 \times 10^{-12}}$	-1.3×10^{-11}	-1.8×10^{-11}	-1.0×10^{-12}	$\mathbf{-1.5 \times 10^{-12}}$	-2.2×10^{-12}	-9.5×10^{-10}	-1.6×10^{-09}	-2.2×10^{-09}	-3.4×10^{-09}	$\mathbf{-3.2 \times 10^{-09}}$	-5.7×10^{-09}
(32) $Propanoate + 3H_2O \rightarrow Acetate + HCO_3^- + H^+ + 3H_2$												
(33) $2CO + O_2 + 2H_2O \rightarrow 2HCO_3^- + 2H^+$	-3.4×10^{-45}	-5.1×10^{-43}	-7.8×10^{-37}	-1.2×10^{-77}	-1.7×10^{-70}	-2.4×10^{-62}	-1.3×10^{-79}	-2.1×10^{-70}	-3.1×10^{-62}	-1.4×10^{-79}	-2.0×10^{-72}	-2.8×10^{-65}
(34) $2H_2 + O_2 \rightarrow 2H_2O$	-3.3×10^{-45}	-4.9×10^{-43}	-7.4×10^{-37}	-7.3×10^{-78}	-1.1×10^{-70}	-1.5×10^{-62}	-1.0×10^{-79}	-1.9×10^{-70}	-3.0×10^{-62}	-1.1×10^{-79}	-1.7×10^{-72}	-2.5×10^{-65}
(35) $Acetate + 2O_2 \rightarrow 2HCO_3^- + H^+$	-2.8×10^{-45}	-4.3×10^{-43}	-6.8×10^{-37}	-3.7×10^{-78}	-6.2×10^{-71}	-1.2×10^{-62}	-2.1×10^{-80}	-7.0×10^{-71}	-1.3×10^{-62}	-2.5×10^{-80}	-3.8×10^{-73}	-6.6×10^{-66}
(36) $CH_4 + 2O_2 \rightarrow HCO_3^- + H^+ + H_2O$	-2.7×10^{-45}	-4.1×10^{-43}	-6.5×10^{-37}	-3.6×10^{-78}	-6.1×10^{-71}	-1.2×10^{-62}	-2.1×10^{-80}	-7.2×10^{-71}	-1.4×10^{-62}	-2.5×10^{-80}	-3.9×10^{-73}	-6.5×10^{-66}
(37) $S + 1.5O_2 + H_2O \rightarrow SO_4^{2-} + 2H^+$												
(38) $S_2O_3^{2-} + 2O_2 + H_2O \rightarrow 2SO_4^{2-} + 2H^+$	-2.2×10^{-45}	-3.3×10^{-43}	-5.1×10^{-37}	-4.4×10^{-78}	-7.4×10^{-71}	-1.3×10^{-62}	-2.5×10^{-80}	-7.7×10^{-71}	-1.4×10^{-62}	-2.2×10^{-80}	-3.4×10^{-73}	-5.1×10^{-66}
(39) $HS^- + 2O_2 \rightarrow SO_4^{2-} + H^+$	-2.5×10^{-45}	-3.8×10^{-43}	-5.9×10^{-37}	-2.8×10^{-78}	-4.9×10^{-71}	-9.4×10^{-63}		-5.1×10^{-71}	-9.7×10^{-63}			
(40) $2HS^- + 2O_2 \rightarrow S_2O_3^{2-} + H_2O$	-2.9×10^{-45}	-4.3×10^{-43}	-6.8×10^{-37}	-1.3×10^{-78}	-2.4×10^{-71}	-5.4×10^{-63}		-2.5×10^{-71}	-5.5×10^{-63}			
(41) $2HS^- + O_2 + 2H^+ \rightarrow 2S + 2H_2O$	-2.4×10^{-45}	-3.5×10^{-43}	-5.3×10^{-37}									
(42) $HS^- + 4Hematite + 15H^+ \rightarrow SO_4^{2-} + 8Fe^{2+} + 8H_2O$	$\mathbf{-7.5 \times 10^{-10}}$	-1.1×10^{-09}	-1.3×10^{-09}	-1.3×10^{-09}	$\mathbf{-2.0 \times 10^{-09}}$	-2.8×10^{-09}	-6.6×10^{-09}	$\mathbf{-1.1 \times 10^{-08}}$	-1.5×10^{-08}	-7.9×10^{-10}	$\mathbf{-1.3 \times 10^{-09}}$	-1.8×10^{-09}
(43) $4Fe^{2+} + O_2 + 10H_2O \rightarrow 4Fe(OH)_3 + 8H^+$												

Microbial redox reactions have been ordered according to their power with the most powerful reactions for the 80 °C brine appearing first. The microbial reaction numbers and column heading numbers refer to Figure 3. The power is not reported for reactions for which the free energy was less negative than -20 kJ mol^{-1}. The values in bold represent the top 10 values.

methanogens, whereas the propionate reaction would be more dependent upon the $P\,H_2$. The oxidation of reduced S compounds by O_2 (reactions (16)–(18), (21) and (25) in Table 7), which were marginally favorable in the highly saline ground water remain endothermic after alteration of the siliclastic mineral assemblage. Given that aerobic S oxidizers are not found in this ground water environment, this does not appear to be a significant detriment. For the dolomite aquifer, the S oxidizing reactions remain exothermic despite the lower pH of the impacted system.
2. Of the microbial reactions that were originally unfavorable prior to injection, the reduction of hematite to Fe^{2+} by oxidation of acetate (reaction (39) in Table 7) and H_2 (reaction (41) in Table 7) are still exothermic due to the reduction in pH from 8 to 7. The abiotic reduction of hematite by oxidation of HS^- (reaction (43) in Table 7) is also energetically favorable.
3. The high CO_2 and HCO_3^- concentrations increased the free energy yield for CO_2 reducing methanogenic and acetogenic reaction (reactions (32) and (37) in Table 7) even after alteration of the aquifer mineral assemblage. An increase in acetogenic activity may rescue the aceticlastic methanogens. The extent to which these two reactions can be used to convert the CO_2 into methane and acetate depends upon whether an abiotically generated source of H_2 can be made available.

The most readily identified impact in Figure 3 on the potential microbial power is from reduction of hematite by HS^- oxidation (Table 8). The power levels were generally larger than in the original ground water systems and because of the reduction of one pH unit in the ground water, microbial Fe(III) reduction reactions were more significant. If sufficient electron donors are available for both biotic and abiotic reactions and sufficient Fe(III) bearing oxides are present in the aquifer (as is usually the case) then these reactions will restore the aquifer's pH to its initial value.

The dolomite aquifer was more severely impacted by the simulated CO_2 injection because the dissolution of the aquifer minerals failed to restore the pH to a range that is more commensurate with the pH ranges of some of the microorganisms. The most effective means of remediating this problem if it occurs in the real world is by the addition of H_2 to stimulate the CO_2 reducing methanogenesis and acetogenesis. If mafic igneous rocks are present that contain Fe bearing clinopyroxene, then the lower pH will automatically stimulate the release of H_2 by the oxidation of this ferrous iron to $Fe(OH)_3$ [38].

Another factor associated with the lower pH produced by CO_2 injection is that it facilitates proton pumping reactions across the cell membrane. Microorganisms need to maintain an internal pH that is 1–2 units less than the external pH in order for the proton pumps to generate ATP. For pH values approaching 8.5–9, this becomes problematic because high internal pH values affect the aqueous species of phosphate making it more difficult to synthesis ATP. The microorganism is then required to expend energy in ion transport across the membrane to correct for this problem. A more neutral pH of 6–7 alleviates this energy drain. The greater availability of energy will also facilitate the fixation of N_2 which would help support growth of the microbial population. The lower pH should also help solubilize phosphate for growth. In aquifers where organic acids are naturally more abundant and the pH typically lower, the impact of CO_2 injection should be less. For aquifers low in organic acids, CO_2 injection will lead to an increase in acetate if a sufficient source of H_2 is available. This in turn should lead to stimulation of overall microbial activity.

For long-term storage of CO_2 the activity of Fe(III) reducing microorganisms will increase the pH and, most likely, lead to the precipitation of various carbonates. Microbial biomass may become concentrated at the gas/water boundary where electron donor/acceptor fluxes will be highest. As readily available Fe(III) is depleted it can be introduced. If this is not feasible and sulfate is not a major constituent in the ground water, then methanogenic activity will begin to dominate and the proportion of CO_2 converted to CH_4 will depend upon the H_2 and acetate fluxes.

For rhizosphere and surface biosphere the most obvious impact would be due to a potential increase in crustal CH_4 flux and a decrease in H_2 flux. Since the fluxes of both gaseous species from fermentative communities in shallower, organic-rich aquitards are 10–100 times greater than the deep subsurface flux, this probably is not a showstopper.

CONCLUSIONS

Based upon the calculated potential microbial power for microbial redox reactions, the most readily identified impact of CO_2 injections on the subsurface microbial communities was the reduction of one pH unit for the ground water hosted in the siliclastic reservoir. The slightly lower pH is based upon the assumption, yet to be verified, that alteration of detrital feldspars to clay in equilibrium with calcite occurs on the time scale of the injection. The power levels for many of the microbial redox reactions were generally larger than in the original ground water systems but because of this reduction of one pH unit in the ground water, microbial Fe(III) reduction reactions were particularly more significant. If sufficient electron donors are available for both biotic and abiotic Fe(III) reducing reactions and sufficient Fe(III) bearing oxides are present in the aquifer (as is usually the case) then these reactions will restore the aquifer's pH to its initial, pre-injection value. CO_2 injection should cause a short term stimulation of Fe(III) reducing communities.

A dolomitic or carbonate aquifer may be more severely impacted by the simulated CO_2 injection because the dissolution of the carbonate failed to restore the pH to a range that is more commensurate with the pH ranges of some of the microorganisms. The most effective means of remediating this problem if it occurs in the real world is by the addition of H_2 to stimulate the CO_2 reducing methanogenesis and acetogenesis. If mafic igneous rocks host the groundwater and contain Fe bearing clinopyroxene, then the lower pH will automatically stimulate the release of H_2 by the oxidation of this ferrous iron to $Fe(OH)_3$ [38]. This in turn would lead to stimulation of methanogenic and acetogenic communities and a reduction of the injected CO_2. Fe(III) reducing microbial reactions may also be stimulated by the appearance of $Fe(OH)_3$ leading to Fe(III) reduction and an eventual increase in pH. The outcome of CO_2 injection in carbonate and mafic rock hosted aquifers is probably the least understood.

Another factor associated with the lower pH produced by CO_2 injection is that it facilitates proton pumping reactions across the cell membrane. Microorganisms need to maintain an internal pH that is 1–2 units less than the external pH in order for the proton pumps to generate ATP. For pH values approaching 8.5–9, this becomes problematic because high internal pH values affect the aqueous species of phosphate making it more difficult to synthesis ATP. The microorganism is then required to expend energy in ion transport across the membrane to correct for this problem. A more neutral pH of 6–7 alleviates this energy drain. The greater availability of energy will also facilitate the fixation of N_2 which would help support growth of the microbial population. The lower pH values should also help solubilize phosphate for growth. Overall CO_2 injection should increase the availability of N and P to microbial communities.

For shallow aquifers where organic acids are naturally more abundant and the pH lower than used in the simulations reported here, the impact of CO_2 injection should be less. For aquifers low in organic acids, CO_2 injection will lead to an increase in acetate through acetogenesis, if a sufficient source of H_2 is available. H_2 can be artificially provided through the introduction of zero valence Fe. This in turn should lead to stimulation of overall anaerobic microbial activity.

For long-term storage of CO_2 in siliclastic reservoirs the short-term enhancement of Fe(III) reducing microorganisms will increase the pH and most likely lead to the precipitation of various carbonates. Microbial biomass may become concentrated at the gas/water boundary where electron donor/acceptor fluxes will be highest. As readily available Fe(III) is depleted it can be introduced. If this is not feasible and sulfate is not a major constituent in the ground water, then methanogenic activity will begin to dominate and the proportion of CO_2 converted to CH_4 will depend upon the H_2 and acetate fluxes.

For rhizosphere and surface biosphere the most obvious impact would be due to a potential increase in crustal CH_4 flux for carbonate and mafic rock hosted aquifers and a decrease in H_2 flux in all cases. Since the fluxes of both gaseous species from fermentative communities in shallower, organic-rich aquitards are 10–100 times greater than the deep subsurface flux, this probably is not a showstopper. Nevertheless, this merits further investigation.

RECOMMENDATIONS

The next phase of modeling will simulate microbial reactions by using the potential microbial power value to select the relative rates among the different microbial redox reactions. Additional observation on the dissolved gas concentrations in an aquifer where CO_2 injection is occurring and comparing those measurements to a similar aquifer where CO_2 injection is not taking place would provide constraints for a model to takes into account the changes in dissolved gas concentrations and its impact on the microbial redox reactions.

In siliclastic aquifers where Fe and Al oxyhydroxides are present, surface protonation reactions may moderate pH changes. This will be included in the next phase of modeling. The next phase of modeling should be combined with kinetic expressions for mineral dissolution at ambient formation conditions to refine the rates of approach to equilibrium compared to the rates of gaseous CO_2 migration and heat advection.

The above analysis predicts changes in the gas and aqueous geochemistry and in the composition of the microbial community in response to CO_2 injection. These predictions could be readily tested by collection and geochemical and 16S rDNA analyses of formation fluids at a CO_2 injection site and control site. This would represent the first critical step in validation of the model's predictions. If the microbial factor turns out to be important, then these observations could also provide the foundation upon which experiments could be performed, initially in the lab, on configuration of the injection stream to enhance optimal microbial activity. Geochemical and 16S rDNA analyses of formation fluids from a CO_2 rich gas reservoir would supply critical observations pertinent to long-term residence of CO_2 and would expand our understanding of the deep subsurface carbon cycle.

ACKNOWLEDGEMENTS

This study was supported by a project subcontract from the US Department of Energy (DOE Contract No. DE-FC26-01NT41145) to BP Corporation North America Inc. I appreciate the efforts and suggestions by Dr Charles A. Christopher in recommending that I undertake such a study.

REFERENCES

1. K. Takai, D.P. Moser, M.F. DeFlaun, T.C. Onstott, J.K. Fredrickson, *Appl. Environ. Microbiol.* **67** (2001) 5750.
2. J. Lippmann, M. Stute, T. Torgersen, D.P. Moser, J. Hall, L.-H. Lihung, M. Borcsik, R.E.S. Bellamy, T.C. Onstott, *Geochim. Cosmochim. Acta* **67** (2003) 4597.
3. J.P. Amend, E.L. Shock, *FEMS Microbiol. Rev.* **25** (2001) 175.
4. T.C. Onstott, T.J. Phelps, T. Kieft, F.S. Colwell, D.L. Balkwill, J.K. Fredrickson, F.J. Brockman, in: J. Seckbach (Ed.), Enigmatic Microorganisms and Life in Extreme Environments, Kluwer, Dordrecht, 1998, p. 489.
5. T.C. Onstott, D.P. Moser, J.K. Fredrickson, F.J. Brockman, S.M. Pfiffner, T.J. Phelps, D.C. White, A. Peacock, D. Balkwill, R. Hoover, L.R. Krumholz, M. Borscik, T.L. Kieft, R.B. Wilson, *Environ. Microbiol.* **5** (2003) 1168.
6. R.J. Parkes, B.A. Cragg, S.J. Bale, J.M. Getliff, K. Goodman, P.A. Rochelle, J.C. Fry, A.J. Weightman, S.M. Harvey, *Nature* **371** (1994) 410.
7. K. Pedersen, J. Arlinger, S. Ekendahl, L. Hallbeck, *FEMS Microbiol. Ecol.* **19** (1996) 249.
8. L.-H., Lin, Radiolytic H_2 and Microbial Communities in the Witwaterstand Basin, PhD in Department of Geosciences, Princeton University, Princeton, 2003, p. 160.
9. B.J. Baker, D.P. Moser, B.J. MacGregor, S. Fishbain, M. Wagner, N.K. Fry, B. Jackson, N. Speolstra, S. Loos, K. Takai, B. Sherwood-Lollar, J.K. Fredrickson, D.L. Balkwill, T.C. Onstott, C.F. Wimpee, D.A. Stahl, *Environ. Microbiol.* **5** (2003) 267.
10. P. Reuter, R. Rubus, H. Wilkes, F. Aeckersberg, F.A. Ruiney, H.W. Jannasch, F. Widdel, *Nature* **372** (1994) 455.

11. J. Beeders, R.K. Nilsen, T. Thorstenson, T. Torsvik, *Appl. Environ. Microbiol.* **62** (1996) 3551.
12. G. Ravot, M. Majot, M.-L. Fardeau, B.K.C. Patel, P. Thomas, J.-L. Garcia, B. Ollivier, *Int. J. Syst. Evol. Microbiol.* **49** (1999) 1141.
13. K. Takai, D.P. Moser, T.C. Onstott, N. Speolstra, S.M. Pfiffner, A. Dohnalkova, J.K. Fredrickson, *Int. J. Syst. Bacteriol.* **51** (2001) 1245.
14. T.L. Kieft, J.K. Frredrickson, T.C. Onstott, Y.A. Gorby, H.M. Kostandarithes, T.J. Bailey, D.W. Kennedy, S.W. Li, A.E. Plymale, C.M. Spadoni, M.S. Gray, *Appl. Environ. Microbiol.* **65** (1999) 1214.
15. D.R. Boone, Y. Liu, Z. Zhao, D.L. Balkwill, G.R. Drake, T.O. Stevens, H.C. Aldrich, *Int. J. Syst. Bacteriol.* **45** (1995) 441.
16. Lovley, *Ann. Rev. Microbiol.* **47** (1993) 263.
17. C.R. Myers, J.M. Myers, *FEMS Microbiol. Lett.* **108** (1993) 15.
18. A.C. Greene, B.K.C. Patel, A.J. Sheehy, *Int. J. Syst. Evol. Microbiol.* **47** (1997) 505.
19. K.O. Stetter, R. Hubert, E. Blochl, M. Kurr, R.D. Eden, M. Fielder, H. Cash, I. Vance, *Nature* **365** (1993) 743.
20. R. Jakobsen, H.-J. Albrechtsen, M. Rasmussen, H. Bay, P.L. Bjerg, T.H. Christensen, *Environ. Sci. Tech.* **32** (1998) 2142.
21. N.L. Plummer, J.F. Busby, R.W. Lee, B.B. Hanshaw, *Water Resour. Res.* **26** (1994) 1981.
22. L.N. Plummer, *Water Resour. Res.* **13** (1977) 801.
23. H.C. Helgeson, A.M. Knox, C.E. Owens, E.L. Shock, *Geochim. Cosmochim. Acta* **57** (1993) 3295.
24. R.K. Thauer, K. Jungermann, K. Decker, *Bacteriol. Rev.* **41** (1977) 100.
25. B. Shink, *Microbiol. Mol. Biol. Rev.* **61** (1997) 262.
26. B.E. Jackson, M.J. McInerney, *Nature* **415** (2002) 454.
27. E.L. Cussler, Diffusion Mass Transfer in Fluid Systems, Cambridge University Press, Cambridge, 1984.
28. T.J. Phelps, E.M. Murphy, S.M. Pfiffner, D.C. White, *Microb. Ecol.* **28** (1994) 335.
29. T.L. Kieft, T.J. Phelps, in: P.S. Amy, D.L. Haldeman (Eds.), The Microbiology of the Terrestrial Deep Subsurface, CRC Lewis Publishers, Boca Raton, FL, 1997, p. 137.
30. J.G. Kuenen, M.S.M. Jetten, *ASM News* **69** (2001) 456.
31. B. Thamdrup, T. Dalsgaard, *Appl. Environ. Microbiol.* **68** (2002) 1312.
32. T. Dalsgaard, B. Thamdrup, *Appl. Environ. Microbiol.* **68** (2002) 3802.
33. T.M. Hoehler, M.J. Alperin, D.B. Alber, C.S. Martens, *Geochim. Cosmochim. Acta* **62** (1998) 1745.
34. D. Haendel, K. Muhle, H.-M. Nitzxche, G. Stiehl, U. Wand, *Geochim. Cosmochim. Acta* **50** (1986) 749.
35. M. Hochman, A Case for Biotic Speliogenesis in a Dolomite Aquifer in South Africa, B.A. Dissertation, in Department of Geosciences, Princeton University, Princeton, 2000, p. 132.
36. D.P. Moser, T.C. Onstott, J.K. Fredrickson, F.J. Brockman, D.L. Balkwill, G.R. Drake, S. Pfiffner, D.C. White, K. Takai, L.M. Pratt, J. Fong, B. Sherwood-Lollar, G. Slater, T.J. Phelps, N. Spoelstra, M. DeFlaun, G. Southam, A.T. Welty, B.J. Baker, J. Hoek, *Geomicrobiol. J.* **20** (2003) 1.
37. B. Sherwood-Lollar, S.K. Frape, S.M. Weise, P. Fritz, S.A. Macko, J.A. Welhan, *Geochim. Cosmochim. Acta* **57** (1993) 5087.
38. T.O. Stevens, J.P. McKinley, *Science* **270** (1995) 450.

This page is intentionally left blank